

2-Amino-9H-pyrido[2,3-b]indole (A $\alpha$ C) Adducts and Thiol Oxidation of Serum Albumin as Potential Biomarkers of Tobacco Smoke

Khyatiben V. Pathak<sup>1</sup>, Medjda Bellamri<sup>2</sup>, Yi Wang<sup>1</sup>, Sophie Langouët<sup>2</sup>, and Robert J. Turesky<sup>1</sup>

<sup>1</sup>Masonic Cancer Center and Department of Medicinal Chemistry, University of Minnesota, Minneapolis, MN 55455, USA

<sup>2</sup>UMR Inserm 1085 IRSET, Rennes1 University, UMS 3480 Biosit, F-35043 Rennes, France

**\*Running title:** *Characterization of A $\alpha$ C-serum albumin adducts*

To whom correspondence should be addressed: Robert J. Turesky, Masonic Cancer Center and Department of Medicinal Chemistry, University of Minnesota, Minneapolis, MN 55455, USA, Tel.: (612) 626-0141; Fax: (612) 624-3869; E-mail: [rturesky@umn.edu](mailto:rturesky@umn.edu)

**Keywords:** Tobacco smoke carcinogens; 2-Amino-9H-pyrido[2-3-b]indole (A $\alpha$ C); Serum Albumin and DNA carcinogen adducts; arylsulfonamide adducts, Cys<sup>34</sup> and Met<sup>329</sup> oxidation

**Background:** The reactivity of A $\alpha$ C, a tobacco smoke carcinogen, was investigated with DNA and albumin of human hepatocytes.

**Results:** Hepatocytes bioactivate A $\alpha$ C to metabolites which adduct to DNA and albumin.

**Conclusion:** Cys<sup>34</sup> and Met<sup>329</sup> of serum albumin are targets for A $\alpha$ C electrophiles.

**Significance:** A $\alpha$ C forms macromolecular adducts and induces oxidative stress, which may be contributing factors to liver damage and cancer risk in smokers.

**ABSTRACT**

2-Amino-9H-pyrido[2-3-b]indole (A $\alpha$ C) is a carcinogenic heterocyclic aromatic amine (HAA) formed during the combustion of tobacco. A $\alpha$ C undergoes bioactivation to form electrophilic N-oxidized metabolites that react with DNA to form adducts, which can lead to mutations. Many genotoxicants and toxic electrophiles react with human serum albumin (albumin); however, the chemistry of reactivity of A $\alpha$ C with proteins has not been studied. The genotoxic metabolites, 2-hydroxyamino-9H-pyrido[2-3-b]indole (HONH-

A $\alpha$ C), 2-nitroso-9H-pyrido[2-3-b]indole (NO-A $\alpha$ C), a N-acetoxy-9H-pyrido[2-3-b]indole (N-acetoxy-A $\alpha$ C), and their [<sup>13</sup>C<sub>6</sub>]-A $\alpha$ C labelled homologues were reacted with albumin. Sites of adduction of A $\alpha$ C to albumin were identified, by data dependent scanning and targeted bottom-up proteomics approaches employing ion trap and Orbitrap MS. A $\alpha$ C-albumin adducts were formed at Cys<sup>34</sup>, Tyr<sup>140</sup> and Tyr<sup>150</sup> residues, when albumin was reacted with HONH-A $\alpha$ C or NO-A $\alpha$ C. Sulfenamide, sulfinamide, and sulfonamide adduct formation occurred at Cys<sup>34</sup> (A $\alpha$ C-Cys<sup>34</sup>). N-Acetoxy-A $\alpha$ C also formed an adduct at Tyr<sup>332</sup>. Albumin-A $\alpha$ C adducts were characterized in human plasma treated with N-oxidized metabolites of A $\alpha$ C and human hepatocytes exposed to A $\alpha$ C. High levels of N-(deoxyguanosin-8-yl)-A $\alpha$ C (dG-C8-A $\alpha$ C) DNA adducts were formed in hepatocytes. The Cys<sup>34</sup> was the sole amino acid of albumin to form adducts with A $\alpha$ C. Albumin also served as an antioxidant and scavenged reactive oxygen species (ROS) generated by metabolites of A $\alpha$ C in hepatocytes: there was a strong decrease in reduced Cys<sup>34</sup> while the levels of Cys<sup>34</sup>sulfinic acid (Cys-SO<sub>2</sub>H), Cys<sup>34</sup>-sulfonic acid (Cys-SO<sub>3</sub>H) and Met<sup>329</sup> sulfoxide were greatly increased. Cys<sup>34</sup>-adduction products and Cys-SO<sub>2</sub>H, Cys-SO<sub>3</sub>H and Met<sup>329</sup> sulfoxide may be potential biomarkers to assess exposure and oxidative

## stress associated with AαC and other arylamine toxicants present in tobacco smoke.

Tobacco smoke is a major risk factor for lung cancer, but also cancer of the liver, bladder, and gastrointestinal tract (1-4). The combustion of tobacco produces many genotoxicants including polycyclic aromatic hydrocarbons, nitrosamines, aromatic amines, and heterocyclic aromatic amines (HAAs), which are potential human carcinogens (5). AαC was originally discovered as a mutagenic pyrolysis product of protein (6) and subsequently identified in cigarette smoke at levels ranging from 60 - 250 ng/cigarette (7,8). These quantities are far greater than those of the aromatic amines 4-aminobiphenyl and 2-naphthylamine, which are implicated in the pathogenesis of bladder cancer in smokers (1,9). Apart from the endocyclic nitrogen atoms, AαC shares the same structure as 2-aminofluorene, one of the most well studied aromatic amine carcinogens (10). Significant levels of AαC were detected in the urine of male smokers of the Shanghai cohort in China, providing evidence that tobacco smoke is a major source of AαC exposure (11). AαC is a liver carcinogen in mice, a transgene colon mutagen and an inducer of colonic aberrant crypt foci, an early biomarker of colon neoplasia (12-14). Therefore, AαC could play a role in the incidence of liver or digestive tract cancers of smokers.

AαC undergoes metabolic activation by N-oxidation of the exocyclic amine group, by cytochrome P450 (P450) enzymes, to form 2-hydroxyamino-9*H*-pyrido[2-3-*b*]indole (HONH-AαC) (Fig.1) (15,16). HONH-AαC can undergo conjugation reactions with *N*-acetyltransferases or sulfotransferases, to form unstable esters. These metabolites undergo heterolytic cleavage to form the proposed short-lived nitrenium ion of AαC (Fig.1) (17), which reacts with DNA to form covalent adducts, leading to mutations (18). The genotoxic potential of AαC has been shown in human peripheral blood lymphocytes (19), Chinese hamster ovary cells (18), and human hepatocytes (20), where high levels of AαC-DNA adducts are formed. However, long-term stable biomarkers of AαC must be developed for implementation in molecular epidemiology studies that seek to address a role for this chemical in human cancer risk.

DNA adducts of AαC can be measured by

sensitive liquid chromatography/mass spectrometry (LC/MS)-based methods (20). However, DNA from biopsy specimens is often unavailable, and restricts the use of this biomarker. The electrophilic N-oxidized metabolites of AαC are also expected to react with proteins (21). The biomonitoring of protein-carcinogen adducts is an alternative approach to assess exposure to hazardous chemicals. Stable carcinogen protein adducts do not undergo repair and are expected to follow the kinetics of the lifetime of the protein (22,23). The major proteins in blood are hemoglobin (Hb) with a life-span of 60 days, and human serum albumin with a half-life of 21 days. The chemistry of reactivity of Hb and albumin with various genotoxicants and toxic electrophiles have been reported (24-26), and several protein-carcinogen adducts have been employed to assess human exposures (23,27,28).

Our goal is to develop and implement protein-based biomarkers of AαC and other HAAs (29,30) in molecular epidemiological studies designed to assess the role of HAAs in human cancers. In this study, we have examined the reactivity of albumin with N-oxidized metabolites of AαC. Cys<sup>34</sup>, followed by Tyr<sup>140</sup> and Tyr<sup>150</sup> of albumin were major sites of adduction of AαC electrophiles. The Cys<sup>34</sup> and Met<sup>329</sup> residues of albumin also served as scavengers of reactive oxygen species (ROS) generated by metabolites of AαC, and the Cys<sup>34</sup> sulfinic acid (Cys-SO<sub>2</sub>H), sulfonic acid (Cys-SO<sub>3</sub>H), and Met<sup>329</sup> sulfoxide were recovered in high yield from human hepatocytes treated with AαC.

## EXPERIMENTAL PROCEDURES

*Caution* — AαC is a potential human carcinogen. AαC and its derivatives must be handled in a well-ventilated fume hood with proper use of gloves and protective clothing.

*Chemicals and Materials*— AαC was purchased from the Toronto Research Chemicals (Toronto, ON, Canada). [4*b*,5,6,7,8,8*a*-<sup>13</sup>C<sub>6</sub>]AαC was a gift from Dr. Daniel Doerge, National Center for Toxicological Research (Jefferson, AR). Albumin, trypsin, chymotrypsin, pronase E, prolidase, leucine amino peptidase, β-mercaptoethanol (βME), iodoacetamide (IAM), dithiothreitol (DTT), acetic anhydride, and Pd/C were obtained from Sigma-Aldrich Chemical Co. (St. Louis, MO). LC-MS grade solvents were from Fisher Scientific (Pittsburg, PA). Tetrahydrofuran

(THF) was obtained from Alfa Aesar (Ward Hill, MA). Amicon Ultra Centrifugal Filters (10 kDa cut off) were purchased from Millipore (Billerica, MA). Pierce albumin depletion kit was purchased from Thermo Scientific (Rockford, IL). Human plasma was purchased from Bioreclamation LLC (Hicksville, NY).

*Synthesis of N-oxidized metabolites of AαC*—2-Nitro-9H-pyrido[2,3-b]indole (NO<sub>2</sub>-AαC) and [<sup>13</sup>C<sub>6</sub>]-NO<sub>2</sub>-AαC were prepared by oxidation of AαC with dimethyldioxirane (17). HONH-AαC and HONH-[<sup>13</sup>C<sub>6</sub>]AαC were prepared by reduction of NO<sub>2</sub>-AαC in THF with hydrazine, using Pd/C as a catalyst (31). HONH-AαC was oxidized to 2-nitroso-9H-pyrido[2,3-b]indole (NO-AαC) with a potassium ferricyanide (32). N-(Deoxyguanosin-8-yl)-AαC (dG-C8-AαC) and the isotopically labeled internal standards [<sup>13</sup>C<sub>10</sub>]-dG-C8-AαC were synthesized as described (33).

*Modification of albumin and human plasma with N-oxidized metabolites of AαC*— Mixed disulfides formed at Cys<sup>34</sup> of commercial albumin (34) were reduced by treatment with βME (35). The reduced albumin was recovered in 100 mM potassium phosphate buffer (pH 7.4) employing Amicon Ultra centrifugal filters. The reduced albumin contained 0.98 mol Cys<sup>34</sup>/mol albumin upon βME treatment. An equimolar solution of HONH-AαC and HNOH-[<sup>13</sup>C<sub>6</sub>]AαC or N-acetoxy-AαC and N-acetoxy-[<sup>13</sup>C<sub>6</sub>]AαC (15 nmol, in 10 μL EtOH) or NO-AαC (30 nmol in 10 μL EtOH) was reacted with albumin (0.6 nmol, 40 μg) in 1 ml of 100 mM potassium phosphate buffer (pH 7.4) at 37 °C for 18 h. N-Acetoxy-AαC and N-acetoxy-[<sup>13</sup>C<sub>6</sub>]AαC were prepared *in situ* by adding the HONH-AαC (15 nmol) to the solution of albumin, immediately followed by the addition of 450 nmol of acetic anhydride (36), and incubated at 37 °C for 1 h. N-Acetoxy-AαC and N-acetoxy-[<sup>13</sup>C<sub>6</sub>]AαC were prepared *in situ* by adding the HONH-AαC (15 nmol) to the solution of albumin, immediately followed by the addition of 450 nmol of acetic anhydride (36), and incubated at 37 °C for 1 h. The unreacted AαC metabolites were removed by ethyl acetate extraction. Human plasma (5 μL, containing ~200 μg of albumin, 3 nmol) was diluted with 1 ml PBS and reacted with N-oxidized AαC derivatives as described above. Albumin from plasma was purified affinity purification by Pierce albumin depletion kit. Other studies on AαC-albumin adduct formation were carried out using lower amounts of N-oxidized

AαC (*vide infra*).

*Human hepatocyte cell culture*— Human samples were obtained from the Centre de Ressources Biologiques (CRB)-Santé of Rennes (<http://www.crbsante-rennes.com>). The research protocol was conducted under French legal guidelines and approved by the local institutional ethics committee. Hepatocytes were isolated by a two-step collagenase perfusion, and the parenchymal cells were seeded at a density of ~ 3 x 10<sup>6</sup> viable cells /19.5 cm<sup>2</sup> Petri dish in 3 mL of Williams' medium with supplements as reported (20), except fetal calf serum was replaced with human albumin pretreated with βME (1 g/L). After two days, the differentiated cells were incubated with AαC (20,33).

*Albumin and DNA adduct formation with AαC in Hepatocytes*— Metabolism studies with AαC (0 or 50 μM in DMSO, 0.01% v/v) were conducted for 24 h. A solution of 1:1 AαC and [<sup>13</sup>C<sub>6</sub>]AαC (50 μM) was employed for characterization of AαC-albumin adducts, whereas the DNA adduct studies employed AαC (50 μM). The culture media containing albumin were removed after 24 h incubation and immediately stored at -80 °C. The cells were washed with PBS and cell pellets were collected by centrifugation a 3500 g for 10 min at 4 °C. Cells were stored at -80 °C until further use. Cell viability was determined by methylthiazol-tetrazolium test and treatment with AαC did not decrease cell viability (37). The media was extracted with 3 vol of ethyl acetate and then the albumin was recovered with >85% purity, by ethanol precipitation. For some analyses, the albumin (100 μg, 1.5 nmol) was alkylated with a 100 molar excess IAM (150 nmol) at 37 °C for 1 h. Excess of IAM was removed by Amicon Ultra centrifugal filters.

*Trypsin/chymotrypsin digestion*— The digestion of AαC-modified albumin (10 μg) was carried out using trypsin and chymotrypsin at protease:protein ratio, respectively, at 1:50 (w/w) and 1:25 (w/w), in 100 μL 50 mM ammonium bicarbonate buffer (pH 8.5) containing CaCl<sub>2</sub> (1 mM) at 37 °C for 16-18 h (35).

*Pronase E/leucine aminopeptidase/prolidase digestion*— albumin (10 μg, 150 pmol) was digested with pronase E, leucine aminopeptidase and prolidase at a protease to protein ratios, respectively, at 1:2 (w/w), 1:30 (w/w) and 1:8 (w/w), in 50 mM ammonium bicarbonate buffer (pH 8.5) containing MnCl<sub>2</sub> (1 mM) at 37 °C for 20 h (23). The AαC-

amino acid adducts were enriched by SPE (32).

*UPLC-Mass Spectrometry Parameters for Peptide Analyses*— Peptides were resolved with an Atlantis C18 nanoACQUITY column (0.3 mm x 150 mm, 3 μm particle size, 100 Å) (Waters Corp., Milford, MA) using Solvent A (5% acetonitrile, 94.99% water, 0.01% formic acid) and Solvent B (95% acetonitrile, 4.99% water, 0.01% formic acid) as mobile phases with Thermo Dionex Ultimate 3000 Nano/Cap LC System connected to an Orbitrap Elite Mass spectrometer (Thermo Scientific, San Jose, CA) using an Advance CaptiveSpray source (Auburn, CA) in the positive ionization mode.

A 60 min gradient (99% A solvent to 60% B solvent for 45 min, 60 to 99% B solvent at 45-60 min) and 25 min gradient (99% A solvent to 60% B solvent for 20 min and 60% to 90% B solvent for 20-25 min) at 5 μL/min flow rate were used, respectively, for data dependent (DDA) and targeted data acquisition.

The top five precursor ions for CID-MS/MS analysis with dynamic exclusion for 180 s with a 3 repeats for 60 s repeat duration were selected for DDA. Mass-tag DDA (MS-tag DDA) was employed to trigger MS/MS on peptides and amino acid adducts displaying characteristic pattern of 1:1 isotopic mixture of AαC and [<sup>13</sup>C<sub>6</sub>]-AαC (40). The partner intensity ratio of 85-100%; *m/z* difference of 6 (singly charged), 3 (doubly charged), 2 (triply charged) species. A mass list of precursor ions (Table 1) for AαC-amino acid and AαC-peptide adducts identified from MS-tag DDA were used for targeted analysis.

The tune parameters were: capillary tube temperature, 270 °C; spray voltage, 2.5 kV; S-lens RF level, 68 (%); in-source fragmentation, 5 V; collision gas, Helium; normalized collision energy, 35 eV; activation Q 0.3; HCD collision gas, Argon; HCD collision energy, 20 - 35. Full scan data were acquired over a mass range of 150-1800 *m/z* at a resolving power of 120,000 (at 400 *m/z*), whereas, MS/MS data acquisition was carried out with the iontrap or Orbitrap (resolving power 60,000) as mass analyzer with isolation widths 1.5, 2. An internal lock mass at *m/z* 371.1012 (polysiloxane) was employed while using the orbitrap mass analyzer. The tune parameters were optimized with LQQCPFEHVK and LQQCPF peptides (New England Peptide, Gardner MA). Mass spectral data were acquired with Xcalibur version 3.0.63 software.

*Data analysis of AαC-albumin* — The BumberDash platform (Version 1.4.115) with Myrimatch search algorithm (Version 2.1.138) with 31 protein subset of RefSeq human protein database, version 37.3, with their forward and reverse protein sequences were used to search for the AαC-peptide adducts (29,38). The dynamic modifications used in Myrimatch configuration file were: oxidation (+15.99 Da) on Met, Cys; deamidation (-17.03 Da) on N-terminal Gln; AαC and [<sup>13</sup>C<sub>6</sub>]-AαC (+181.06 and 187.11) on Cys, Lys, Tyr, Ser, Thr, Trp, His, Glu, Asp; SO-AαC and SO-[<sup>13</sup>C<sub>6</sub>]-AαC (+197.06, +203.10) on Cys and SO<sub>2</sub>-AαC and SO<sub>2</sub>-[<sup>13</sup>C<sub>6</sub>]-AαC (+213.05, +219.10); acetylation (+42.01) on Lys, Cys, Tyr, Arg. The search parameters used were: enzyme (trypsin/chymotrypsin), up to two missed cleavages, mass tolerances 1.25 *m/z* (precursor ions) and 0.5 *m/z* (product ions). Each identified spectrum was filtered by IDPicker algorithm (Version 3.0.564) with a false discovery rate (FDR) (1%). The peptide sequence of identified AαC-peptide and AαC-monoamino acid adducts was confirmed by manually sequencing.

*DNA isolation and UPLC/MS<sup>3</sup> measurement of AαC-DNA adducts*— DNA was isolated by the phenol/chloroform method (20). DNA (5 μg) was spiked with the isotopically labeled internal standard ([<sup>13</sup>C<sub>10</sub>]-dG-C8-AαC) at 1 adduct per 10<sup>6</sup> bases, followed by enzymatic digestion of DNA (39). The UPLC /MS<sup>3</sup> measurement of AαC-DNA adducts were performed using a NanoAcquity UPLC system (Waters Corp., New Milford, MA) coupled with LTQ VelosPro ion-trap mass spectrometer (Thermo Fisher, San Jose, CA) as described previously (42). The ions were monitored with the MS<sup>3</sup> scan mode. For dG-C8-AαC, ions at *m/z* 449.1 (MS) > 333.1 (MS<sup>2</sup>) > 209.2, 291.4, 316.4 (MS<sup>3</sup>) and for the internal standard, [<sup>13</sup>C<sub>10</sub>]-dG-C8-AαC, ions at *m/z* 459.1 (MS) > 338.1 (MS<sup>2</sup>) > 210.2, 295.4, 321.5 (MS<sup>3</sup>) were monitored (40).

## RESULTS

The metabolic activation of AαC in hepatocytes, and reaction of N-oxidized AαC metabolites with DNA and albumin, and the scavenging of ROS by albumin are summarized in Fig. 1.

The UV spectra of AαC, HONH-AαC, and NO-AαC are displayed in Fig 2A. NO-AαC displays a redshift in its maximal absorbance compared to

AαC and HOHN-AαC. The product ion spectrum of AαC ( $[M+H]^+$  at  $m/z$  184.1) displays fragment ions at  $m/z$  167.0 and 157.1, attributed to the loss of  $NH_3$  and HCN (Fig 2B) (9). The product ion spectrum of NO-AαC ( $[M+H]^+$   $m/z$  198.1) displays a sole ion at  $m/z$  168.0 and assigned to the loss of the NO group (Fig 2C). The product ion spectrum of HONH-AαC ( $[M+H]^+$  at  $m/z$  200.1) displays prominent fragment ions at  $m/z$  182.1 and 183.1, which are attributed to the losses of  $H_2O$  and  $OH^\bullet$ , and the product ion at  $m/z$  155.1 is attributed to a loss of  $H_2O$  and HCN (Fig 2D).

*MS-tag DDA mapping of AαC-albumin peptides and AαC-amino acid adducts*— The assignment of AαC-peptide adducts are based on CID and higher-energy collision dissociation (HCD) tandem MS.

The chromatograms of the MS-tag DDA experiments of albumin modified with a 50-fold molar excess of N-oxidize AαC and  $[^{13}C_6]A\alpha C$  (1:1 ratio) were filtered using  $m/z$  values of the isotopic pair, i.e. for the radical cation ( $A\alpha C^{\bullet+}$  at  $m/z$  183.1,  $[^{13}C_6]A\alpha C^{\bullet+}$  at  $m/z$  189.1) and protonated ions ( $A\alpha C^+$  at  $m/z$  184.1 and  $[^{13}C_6]A\alpha C$  at  $m/z$  190.1). (Fig. 3). Nine AαC-peptide adducts (P1-P9) were detected in the tryptic/chymotryptic digest. The assignments of the peptide adduct sequences and accurate mass measurements of the amino acid adducts, following digestion with pronase E, leucine aminopeptidase, and prolidase, are listed in Table 1. Cys<sup>34</sup>, followed by Tyr<sup>140</sup> and Tyr<sup>150</sup> formed adducts with HONH-AαC; an additional adduct was formed at Tyr<sup>332</sup> with *N*-acetoxy-AαC. The adduction of NO-AαC primarily occurred at Cys<sup>34</sup>, followed by much lower levels of adduct formation at Tyr<sup>150</sup>.

*MS characterization of adducts formed at Cys<sup>34</sup> of albumin*- The digestion of AαC-modified albumin with trypsin/chymotrypsin produced peptides containing adducts at  $^{31}LQQC*PF^{36}$ ,  $^{32}QQCPFEDHVK^{41}$  and  $^{31}LQQCPF EDHVK^{41}$ . A total of six adducts with different oxidation states of the sulfur atom were identified. The product ion spectra of several adducts peptides are described in detail below. *LQQ\*CPFEDHVK-AαC adducts*— The single missed cleavage peptide containing the proposed sulfonamide adduct  $LQQ*C^{[SO_2A\alpha C]}PF EDHVK$  (P2) (1555.7 Da), eluted at  $t_R = 17.7$  min and occurred as a triply charged species  $[M+3H]^{3+}$  at  $m/z$  519.6 (Fig. 4A). The 213 Da increase in mass

over the non-modified peptide corresponds to the addition of AαC (182), and two oxygen atoms (32) minus one proton (1) on the -SH moiety. The product ion spectrum of  $m/z$  519.6 displayed a series of -*b* ions and -*y* ions confirming the sequence assignment. The shift in masses at the  $*b_4$  and  $(*y_8)^{2+}$  ions identify the site of adduction at the Cys<sup>34</sup> residue. The proposed sulfonamide adduct  $LQQ*C^{[SO_2A\alpha C]}PF EDHVK$  (P3) (1539.7 Da) at  $t_R = 17.8$  min occurred as a triply charged species  $[M+3H]^{3+}$  at  $m/z$  514.2, a mass 16 Da less than the sulfonamide adduct. The product ion spectrum of  $m/z$  514.2 contains minor fragment ions at  $m/z$  183.1 ( $A\alpha C^{\bullet+}$ ) and 184.1 ( $A\alpha C^+$ ), with a base peak at  $m/z$  679.9, corresponding to the sulfonium ion  $[M+2H-A\alpha C]^{2+}$  (Fig. 4B). The MS<sup>3</sup> scan stage product ion spectrum of the proposed  $LQQ*C^{[SO]}PFEDHVK$  sulfoxide ion at  $m/z$  679.9 [M'] showed -*b* and -*y* ions series in MS<sup>3</sup> scan stage product ion spectrum at  $m/z$  679.9 [M'] supports  $LQQ*C^{[SO]}PFEDHVK$  sulfoxide structure. Doubly charged product ion at  $m/z$  648.9 attributed to the loss of  $CH_2SO$  from the M' ion and  $*b_4-SO$ ,  $*b_5$ ,  $*y_8$  and  $*y_9$  ions support the proposed structure (Fig. 4C).

*LQQ\*CPF-AαC peptide adducts*— Three additional S-N linked peptide adducts were identified. The product ion mass spectra of the doubly protonated ions are consistent with the AαC sulfonamide  $LQQ*C^{[SO_2A\alpha C]}PF$  (P4) ( $[M+H]^+$  at  $m/z$  948.4,  $[M+2H]^+$  at  $m/z$  474.7  $t_R$  17.9 min) (Fig. 4D), AαC sulfonamide  $LQQ*C^{[SOA\alpha C]}PF$  (P7) ( $[M+H]^+$  at  $m/z$  932.4,  $[M+2H]^+$  at  $m/z$  466.7  $t_R$  20.4 min) (Fig. 4E-F), and AαC sulfenamide  $LQQ*C^{[A\alpha C]}PF$  (P8) ( $[M+H]^+$  at  $m/z$  916.4,  $[M+2H]^+$  at  $m/z$  458.7  $t_R$  21.5 min) (Fig. 4G).

The doubly charged peptide precursor ion  $[M+2H]^{2+}$  of  $LQQ*C^{[A\alpha C]}PF$  (P8)  $[M+H]^+$  at  $m/z$  458.7 is a 181 Da increase in mass over the non-modified protonated peptide ( $m/z$  735.3). This increase in mass corresponds to the addition of AαC (182) minus one proton (1) from the -SH moiety. The increase in mass of the peptide is consistent with the proposed sulfenamide linkage. The product ion spectrum of  $[M+2H]^{2+}$  at  $m/z$  458.7 (Fig. 4G) shows the -*b* ion and -*y* ion series, where  $*b_4$ ,  $*y_3$ - $*y_5$  ions provide evidence that adduction of AαC occurred at the sulfhydryl group of Cys<sup>34</sup>. The product ion at  $m/z$  439.3 ( $*b_4$ -AαC-SH) occurs via the cleavage of the C-S bond (41,42). The

prominent base peak observed at  $m/z$  184.1 is attributed to protonated AαC (Fig. 4G). It is noteworthy that most arylsulfenamide adducts undergo hydrolysis during proteolytic digestion, which generally makes these adducts difficult to detect (30,43,44).

*MS characterization \*Cys-AαC adducts*—The Cys sulfenamide and sulfinamide linked adducts of AαC underwent hydrolysis to produce AαC during proteolysis of albumin with pronase E, leucine aminopeptidase, and prolidase. Two peaks attributed to Cys-AαC adducts containing the S-dioxide linkage were identified ( $t_R = 10.9$  and 11.5 min) (A1) in the UPLC/MS chromatogram (Fig. 5A-B). The precursor ions  $[M+H]^+$  were observed at  $m/z$  335.0806, a value which is within 0.6 ppm of the calculated  $m/z$  value of the proposed sulfonamide structure (Table 1). The adducts were present in an approximate ratio of 4:6 in albumin modified with HONH-AαC, and a 2:8 ratio when albumin was modified with *N*-acetoxy-AαC (Fig. 5A-B). The adducts were formed at ~5 fold higher levels in albumin treated with *N*-acetoxy-AαC than albumin treated with HONH-AαC. The earlier eluting isomer underwent CID to preferentially form a radical cation at  $m/z$  183.0790 (AαC<sup>•+</sup>), whereas the second adduct favored the formation of the even electron ion at  $m/z$  184.0867, the  $m/z$  of protonated ion of AαC<sup>+</sup> (Fig. 5C-D, Table 2). Other notable product ions were detected for both adducts but with different relative abundances:  $m/z$  230.0382 ( $[AαC+SO]^+$ );  $m/z$  254.0922 ( $[M+H-NH_3-SO_2]^+$ );  $m/z$  271.1189 ( $[M+H-SO_2]^+$ ); and  $m/z$  318.0547 ( $[M+H-H_2O]^+$ ) (Fig. 5C-D, Table 2).

Arylsulfonamides are weak acids and the nitrogen anion of the sulfonamide linkage can form several tautomeric forms with hindered rotation about the S=N bond (45). However, the prominent differences in the product ion spectra combined with the inability to interconvert these Cys-AαC adducts at elevated temperature, suggest that the adducts are not conformational isomers.

The nitrenium ion of HONH-AαC can undergo charge delocalization to form the carbenium ion resonance form with electron deficiency centered at the C-3 position of the AαC skeleton (Fig. 5E) (46). We propose that one isomeric Cys-AαC adduct contains an S-N linkage, and the second adduct

contains a thioether linkage, formed between Cys<sup>34</sup>-SH group and possibly the C-3 atom of AαC (46). The S-N sulfenamide (or sulfinamide) and thioether adducts undergoes oxidation, by ROS generated by aerobic oxidation of N-oxidized AαC metabolites (Fig. 1) or during proteolysis, to form the sulfonamide and sulfone linkages (Fig. 5E) (47). Both adducts undergo CID to form the proposed sulfonium ion at  $m/z$  230.0385 (Fig. 5F)). These adducts were not chromatographically resolved in the tryptic/chymotryptic digests of albumin. Large scale syntheses and NMR studies are required to elucidate the respective structures of these AαC-Cys-S-dioxide linked isomers. The Cys<sup>34</sup> of albumin was reported to react with *N*-acetyl-*p*-benzoquinoneimine, the electrophilic metabolite of acetaminophen and formed two regioisomeric adducts (41).

*MS characterization of adducts formed at Tyr<sup>140,150,332</sup> of albumin*—Three adducts were formed between Tyr residues of albumin and AαC (Table 1).

*L\*YEIAR peptide adduct*—The product ion spectrum of the L\*YEIAR (P5) adduct with a doubly charged peptide precursor ion  $[M+2H]^{2+}$  at  $m/z$  473.3 ( $t_R = 14.1$  min) displayed a series of *-b* ions and *-y* ions [identifies the sequence as <sup>139</sup>L\*Y<sup>[AαC]</sup>EIAR<sup>144</sup> with the site of adduction at Tyr<sup>140</sup> (Fig. 6A). The ion at  $m/z$  763.4 is proposed to arise by the loss of AαC as a radical cation at  $m/z$  183.1  $[M+H-AαC]^+$ , followed by the neutral loss of quinone methide (106.1 Da)  $[M+H-AαC-C_7H_6O]^+$  to form the ion at  $m/z$  657.4 (Fig. 6B). The mass spectral data support the proposed structure as an O-linked adduct formed between oxygen atom of Tyr and possibly the C-3 atom of the heterocyclic skeleton of AαC (46). Further support for the proposed O-linkage is provided by the lower region of the HCD mass spectrum: ions are observed at  $m/z$  183.0790 ( $m/z$  183.0791, calculated) and  $m/z$  199.0745 ( $m/z$  199.0741, calculated) and attributed to, respectively,  $[AαC]^+$  and  $[AαC+O]^+$  (Fig. 6A-B). We recently reported a similar mechanism of fragmentation of an O-linked adduct formed between tyrosine and the HAA 2-amino-1-methyl-6-phenylimidazo[4,5-*b*]pyridine (PhIP) (32).

*MS characterization of an O-linked Tyr-AαC adduct*—The proteolysis of albumin adducts with pronase E, leucine aminopeptidase, and prolidase

produced two Tyr linked adducts of AαC. A first set of Tyr-AαC and Tyr- $^{13}\text{C}_6$ AαC adducts (A2) were observed at  $m/z$  363.1449 ( $m/z$  363.1451, calculated) and  $m/z$  369.1629 ( $m/z$  369.1631, calculated) were observed at  $t_R$  11.8 min. The product ion spectrum of the unlabelled Tyr-AαC adduct  $[\text{M}+\text{H}]^+$  at  $m/z$  363.1449 displayed fragment ions at  $m/z$  346.1186, 317.1395, and 302.1285 attributed, respectively, to the losses of  $\text{NH}_3$ ,  $\text{H}_2\text{CO}_2$ , and  $\text{NH}_3$  and  $\text{CO}_2$  (Fig. 6C, Table 2). The product ions at  $m/z$  289.1210  $[\text{M}+\text{H}-\text{C}_2\text{H}_5\text{NO}_2]^+$  and 288.1137  $[\text{M}+\text{H}-\text{C}_2\text{H}_4\text{NO}_2]^+$  are proposed to arise by cleavage of the  $\text{C}^\alpha$  and  $\text{C}^\beta$  bond of tyrosine. The fragment ion at  $m/z$  183.0791 is assigned to  $\text{A}\alpha\text{C}^{\bullet+}$ , and the ion at  $m/z$  198.0659 is tentatively assigned as the protonated ion of the 2-imino-3-oxo derivative of AαC, with the loss of phenylalanine (165.0790 Da) as a neutral fragment. The ion at  $m/z$  198.0659 provides evidence that adduct formation occurred between the 4-HO group of tyrosine and the AαC heterocyclic ring (Fig. 6D).

*F\*YAPPELL-AαC adducts*— Two minor Tyr adducts of AαC with the peptide sequence  $^{149}\text{F}^*\text{Y}^{[\text{A}\alpha\text{C}]}\text{APELL}^{155}$  (P9A, P9B Fig. 3, Table 1) were identified at  $t_R$  14.5 and 15.8 min (Fig. 7A). The full scan spectra of both adducts displayed doubly charged  $[\text{M}+2\text{H}]^{2+}$  at  $m/z$  517.3. The CID fragment ions of  $m/z$  517.3 displaced the same characteristic  $-b$  ion and  $-y$  ion series attributed to the  $\text{F}^*\text{Y}^{[\text{A}\alpha\text{C}]}\text{APELL}$  for both peptide adducts (Fig. 7A, CID). The shift in mass between the  $y_5$  and  $*y_6$  ion series proves that the site of AαC adduction occurred at Tyr<sup>150</sup> for both peptides (Fig. 7A). CID did not provide appreciable fragment ions at the low  $m/z$  region for either adduct. The doubly protonated ions  $[\text{M}+2\text{H}]^{2+}$  at  $m/z$  517.3 were subjected to HCD to examine for potential fragmentation of the bond formed between the Tyr and AαC. The extracted ion chromatograms were generated at  $m/z$  183.0791 and  $m/z$  184.0869 (Fig. 7A, HCD). The earlier eluting adduct (P9A) at  $t_R$  14.5 min displayed a prominent fragment ion at  $m/z$  184.0869, an ion attributed to protonated AαC (Fig. 7A, HCD at  $t_R$  14.5). The linkage of this adduct may have occurred between the C-3 or C-5 atom of the Tyr phenyl ring and the exocyclic amino group of AαC. The HCD product ion spectrum of the second adduct (P9C) at  $t_R$  15.8 min showed a mixture of product ions assigned as the radical cation of  $\text{A}\alpha\text{C}^{\bullet+}$  and protonated AαC, respectively, at  $m/z$  183.0789 and  $m/z$  184.0868 (Fig. 7A, HCD at  $t_R$  15.8). A Tyr

linkage may have formed at the C-3 or C-7 atom of the heterocyclic ring of AαC, based on studies of nucleophilic trapping agents adducting at these sites of the nitrenium ion of AαC (46,48).

*MS characterization an amine-linked AαC Tyr adduct*— The second set of Tyr-AαC and Tyr- $^{13}\text{C}_6$ -AαC adducts (A3) eluted at  $t_R$  12.1 min (Fig. 7B). The protonated ions  $[\text{M}+\text{H}]^+$  were observed, respectively at  $m/z$  361.1293 and  $m/z$  367.1475, a mass 2 Da less than the Tyr-AαC and Tyr- $^{13}\text{C}_6$ -AαC adducts ( $m/z$  363.1449 and  $m/z$  369.1631) described above (Fig. 7B, Table 2). The structure of the adduct is proposed to be a quinoneimine linked adduct, which occurs by oxidation of P9A (Fig 7B) during proteolytic digestion with the three enzyme mixture. The product ion spectrum of  $[\text{M}+\text{H}]^+$  at  $m/z$  361.1293 shows ions at  $m/z$  344.1025, 315.1239, and 300.1130, which are of losses of, respectively,  $\text{NH}_3$ ,  $\text{H}_2\text{CO}_2$ , and  $\text{NH}_3$  and  $\text{CO}_2$  (Fig. 7B, Table 2). The product ion at  $m/z$  288.1129 is proposed to arise following ring-opening of the protonated quinoneimine ring (Fig. 7C). The Tyr- $^{13}\text{C}_6$ -AαC adduct displays the same product ions as the unlabeled adduct but shifted by 6  $m/z$ .

A third peptide adduct formed between AαC and Tyr was observed only in the albumin modified with *N*-acetoxy-AαC. The CID-MS/MS spectrum of doubly charged protonated precursor ion at  $m/z$  616.8 at 19.3 min displayed typical  $-b$  and  $-y$  ion pattern attributing to LGMFL\*Y $^{[\text{A}\alpha\text{C}]}$ EY (P6) with AαC adduction at Tyr<sup>332</sup> (Supplemental Fig. S1, upper panel). The  $^{13}\text{C}_6$  homologue of this adduct at  $m/z$  619.8 displayed the same pattern of fragmentation (Supplemental Fig. S1 lower panel).

*AαC-SA adduct formation as a function of concentration of N-oxidized AαC metabolites*— The LQQ\*C $^{[\text{SOA}\alpha\text{C}]}$ PFEDHVK (P3) sulfonamide adduct at Cys<sup>34</sup> accounted for 73-80% of the total ion counts of AαC-peptide adducts, when commercial albumin was reacted with a 50-fold molar excess of *N*-oxidized AαC metabolites. *In vivo*, the exposure to AαC occurs at much lower levels than the physiological concentration of albumin, and relative abundances of adducts formed may be different from those adducts formed at elevated exposures to AαC in vitro. Therefore, albumin was treated with HONH-AαC or *N*-acetoxy-AαC over a million fold range of carcinogen per mol albumin (1 to  $10^6$ ) (Fig.

8A-B). We also examined the effect of plasma matrix components on the reactivity of albumin with N-oxidized AαC metabolites. Representative UPLC-MS chromatograms of the peptide adducts recovered from commercial albumin or albumin in plasma modified with 1 molar equivalent of *N*-acetoxy-AαC are shown in Supplemental Fig. 2SA-B.

The Tyr-peptide adducts of AαC at Tyr<sup>140, 150, 332</sup> residues were only detected when albumin was reacted with  $\geq 0.01$  mol *N*-acetoxy-AαC per mol albumin. In contrast, adducts were still formed at Cys<sup>34</sup> with  $1 \times 10^{-5}$  molar ratio of *N*-acetoxy-AαC:albumin (Fig. 8A-B), and LQQ\*C<sup>[SOAαC]</sup>PFEDHVK sulfinamide was the major adduct. The amounts of AαC-peptide adducts formed were ~5-40 times higher in reactions of albumin conducted with *N*-acetoxy-AαC than those amounts of albumin adducts formed with HONH-AαC (Figure 8A-B). The level of AαC adduct formation with albumin in plasma was several fold lower than adduct levels formed with commercial albumin (data not shown). Plasma albumin adducts were not detected at Tyr<sup>140, 150, 332</sup> residues at any concentration of N-oxidized AαC, and the sulfinamide LQQ\*C<sup>[SOAαC]</sup>PFEDHVK was the predominant adduct.

*AαC-DNA and AαC-albumin adduct formation in human hepatocytes*— Reactive N-oxidized intermediates of AαC are formed and adduct to DNA in human hepatocytes and albumin in human hepatocytes (Fig. 1) (20,33). The basal activities of P450 1A1 and 1A2, two major isoforms involved in N-oxidation of AαC (16,17), were measured in human hepatocytes from three donors using ethox-yresorufin and methoxyresorufin as substrates (33). The level of dG-C8-AαC adduct formation from the two donors (A and C) with the highest P450 1A1 and 1A2 activities produced higher levels of dG-C8-AαC than donor B with low enzyme activity (Fig. 9A).

The mass chromatograms of AαC-albumin peptide adducts, following tryptic/chymotryptic digestion of albumin recovered from hepatocytes are shown in Fig. 9B. The relative ion abundances of the peptide adducts are summarized in Fig 9C and product ion spectra are presented in Supplemental Fig 3S. The major adduct, based on ion counts, is LQQ\*C<sup>[SOAαC]</sup>PFEDHVK sulfinamide, followed by LQQ\*C<sup>[SOAαC]</sup>PF, and LQQ\*C<sup>[AαC]</sup>PF. The

occurrence of the LQQ\*C<sup>[SOAαC]</sup>PFEDHVK as the major adduct in hepatocytes is similar to the findings of commercial albumin and albumin in plasma treated with N-oxidized AαC metabolites (Fig. 7A, Fig. 8A, Fig. 9B,C). The LQQ\*C<sup>[AαC]</sup>PF sulfenamide and LQQ\*C<sup>[SOAαC]</sup>PF sulfinamide were also identified, but occurred at lower ion abundances (Fig. 9B,C, Supplemental Fig. 3SA-C). LQQ\*C<sup>[SO<sub>2</sub>AαC]</sup>PF and LQQ\*C<sup>[SO<sub>2</sub>AαC]</sup>PFEDHVK were not detected.

In the absence of stable, isotopically labelled internal standards, quantitative peptide adduct measurements and correlations to DNA adduct levels of AαC cannot be determined. However, the ion counts of the major albumin peptide adduct, LQQ\*C<sup>[SOAαC]</sup>PFEDHVK sulfinamide were greatest in donor C who also harbored the highest level of dG-C8-AαC (Fig. 9A-B,C). Very high levels of AαC also were recovered in all of the hepatocytes (Fig. 9B,C). The occurrence of AαC is attributed to hydrolysis of S-N linked albumin-AαC adducts during proteolysis and not to unmetabolized AαC bound to albumin, because the isolation procedure effectively removed all unbound AαC from albumin in the cell culture media (Unpublished observations, K. Phatak).

*Oxidative status of albumin-Cys<sup>34</sup> and albumin-Met<sup>329</sup> in human hepatocytes exposed to AαC*— N-Oxidized metabolites of arylamines generate reactive oxygen species (ROS) (49). We sought to determine if AαC had induced oxidative stress in hepatocytes by identification of oxidation products of Cys<sup>34</sup> and Met residues of albumin (50-52). The oxidized sulfinic LQQ\*C<sup>[SO<sub>2</sub>H]</sup>PF and sulfonic LQQ\*C<sup>[SO<sub>3</sub>H]</sup>PFEDHVK acids of Cys<sup>34</sup> of albumin were monitored (29,32), and LQQCPF was measured following derivatization of albumin with iodoacetamide (IAM) (29). Elevated levels of the protonated [M+H]<sup>2+</sup> peptides for LQQ\*C<sup>[SO<sub>2</sub>H]</sup>PFEDHVK at *m/z* 688.3 and LQQ\*C<sup>[SO<sub>3</sub>H]</sup>PFEDHVK at *m/z* 696.3 (29) were detected in all three sets of hepatocytes treated with AαC (Fig 9D). The product ion spectra at *m/z* 688.3 and *m/z* 696.3 displayed typical *-b* and *-y* ion series type fragment ions (Supplemental Fig.4S A-B) and permitted the assignments as the peptide sequences of the Cys sulfinic and sulfonic acids (29). The levels LQQ\*C<sup>[SO<sub>2</sub>H]</sup>PFEDHVK and LQQ\*C<sup>[SO<sub>3</sub>H]</sup>P



FEDHVK in AαC/[<sup>13</sup>C<sub>6</sub>]AαC-treated hepatocytes were, respectively, 6 - 8 and 4 - 6 times higher than the levels in untreated controls, and the levels of IAM-derivatized LQQ\*CPF were decreased by more than 10-fold in AαC-treated hepatocytes (Fig. 9B,D). Myrimatch search for oxidation sites in albumin also identified oxidation at Met<sup>329</sup> residue of albumin. The product ion spectrum of, trypsin/chymotryptic peptide DVFLGM<sup>[O]F</sup> at [M+H]<sup>+</sup> at *m/z* 844.4 representing Met<sup>329</sup> oxidation resulted in typical *-b* and *-y* type of fragment ions where, *-\*y*<sub>2</sub>-*\*y*<sub>6</sub> and *-\*b*<sub>6</sub> product ions further confirmed oxidation at Met<sup>329</sup> (Supplemental Fig. 4SC). From targeted analysis, the level of DVFLGM<sup>[O]F</sup> was ~6 times higher in AαC/[<sup>13</sup>C<sub>6</sub>]AαC-treated hepatocytes than in untreated hepatocytes (Fig. 9B,D).

## DISCUSSION

Primary human hepatocytes are an ideal *ex-vivo* model system for studying metabolism, bioactivation and mechanisms of toxicity of carcinogens, because cofactors are present at physiological concentrations and biotransformation pathways may closely simulate those which occur *in vivo* (53). In this study, we investigated the metabolic activation of AαC, a rodent liver carcinogen, in human hepatocytes, and examined the reactivity of its genotoxic N-oxidized metabolites of AαC with DNA and albumin. Our goal is to develop and implement albumin-based biomarkers of AαC and other HAAs in molecular epidemiological studies designed to assess the role of HAAs in human cancers (54). The Cys<sup>34</sup> residue was the major nucleophilic site of albumin to form adducts with AαC, followed by Tyr<sup>140</sup> and Tyr<sup>150</sup>, which formed adducts at minor levels. Another HAA, PhIP (55), also primarily formed adducts at the Cys<sup>34</sup> of albumin with considerably lower levels of adducts occurring at Tyr<sup>140</sup> and Tyr<sup>150</sup> (56). In contrast, the Tyr<sup>140</sup> and Tyr<sup>150</sup> residues of albumin are the preferred site for adduct formation of neurotoxic organophosphate compounds (57-59).

The preliminary characterization AαC-albumin adducts was performed *in vitro*. The formation of AαC-albumin adducts was greatly enhanced by the *in situ* generation of *N*-acetoxy-AαC, a reactive intermediate of HONH-AαC, which undergoes heterolytic cleavage to produce the nitrenium ion (48). *N*-Acetoxy-AαC is a penultimate

metabolite of AαC that adducts to DNA and proteins (17). The *N*-acetoxy intermediates of HON-AαC, and other *N*-hydroxylated HAAs, such as 2-hydroxyamino-3-methylimidazo[4,5-*f*]quinoline and 2-hydroxyamino-3,8-dimethylimidazo[4,5-*f*]quinoxaline are unstable and cannot be isolated (60). However, the *in situ* formation of these *N*-acetoxy intermediates in the presence of DNA, by reaction of the *N*-hydroxylated HAAs with acetic anhydride, increased the levels of DNA adducts by 10 to 30 fold (36,61,62). Using a similar reaction scheme, we showed that adduct formation of HON-AαC with albumin was also greatly enhanced by the *in situ* generation of *N*-acetoxy-AαC (Fig. 8A-B). The Lys, Arg, Cys, and Tyr residues of albumin can potentially compete with HONH-AαC and undergo acetylation with acetic anhydride and influence the formation of different AαC-albumin adducts. However, the same AαC-albumin adducts were formed by reaction of albumin with a 50 mol excess of HONH-AαC, NO-AαC, or *N*-acetoxy-AαC generated *in situ* (Table 1). Moreover, the Myrimatch search engine did not detect acetylation at Lys, Arg, Cys, or Tyr residues of albumin under these reaction conditions (100 mM potassium phosphate buffer (pH 7.4, 37 °C). Under low reaction conditions with HONH-AαC (10,000:1; albumin:HONH-AαC), the levels of Cys<sup>34</sup> adducts were 50-fold greater when albumin was reacted with HONH-AαC in the presence of acetic anhydride than by reaction of albumin with HONH-AαC alone; thereby, demonstrating that *N*-acetoxy-AαC is efficiently formed *in situ* and readily reacts with nucleophilic sites of albumin to form covalent adducts (Fig. 8A-B).

Human hepatocytes efficiently bioactivated AαC to electrophilic N-oxidized metabolites, which formed covalent adducts with DNA and albumin (Fig. 9). The DNA adduct, dG-C8-AαC, was formed at relatively high levels, ranging from 2 – 12 adducts per 10<sup>6</sup> DNA bases, consistent with our previous data (20,33). dG-C8-AαC was also previously identified in salivary DNA of smokers (63). The Cys<sup>34</sup> residue was the sole site of albumin found to form adducts with AαC metabolites in hepatocytes: both sulfenamide and sulfinamide adducts were identified. However, the ion counts of AαC recovered from the albumin digest were 100-fold or greater than the ion counts of any of the AαC-Cys adducts. These findings signify that a large

proportion of the S-N linked sulfinamide adducts LQQ\*C<sup>[SOAαC]</sup>P FEDHVK and LQQ\*C<sup>[SOAαC]</sup>PF, or the sulfenamide adduct LQQ\*C<sup>[AαC]</sup>PF of albumin underwent hydrolysis during proteolysis. In the absence of stable peptide adducts, or isotopically labeled LQQ\*C<sup>[SOAαC]</sup>PFEDHVK peptides for internal standards, it is difficult to determine the relative reactivity of N-oxidized AαC metabolites with DNA and albumin in hepatocytes.

HONH-AαC and NO-AαC undergo redox cycling in hepatocytes and produce ROS (Fig. 1) (49,64). Previous studies reported that structurally related aromatic amines, some of which are present in tobacco smoke (65,66), deplete glutathione levels in liver or ex-vivo in hepatocytes of rodents and induce oxidative DNA damage (67-69); however, the oxidation of albumin was not reported in those studies. In our study, we show that albumin scavenges ROS produced by metabolites of AαC in human hepatocytes by formation of the oxidized Cys<sup>34</sup> containing peptides LQQ\*C<sup>[SO<sub>2</sub>H]</sup>PFEDHVK, LQQ\*C<sup>[SO<sub>3</sub>H]</sup>PFEDHVK, and the methionine oxidation peptide, DVFLGM<sup>[O]</sup>F. The level of Cys<sup>34</sup> of albumin alkylated with IAM prior to proteolytic digestion decreased by more than 90% in hepatocytes treated with AαC and provides strong evidence that Cys<sup>34</sup> of albumin is scavenging ROS (Fig. 9C). Together with Cys<sup>34</sup>, six Met residues of albumin display antioxidant activity towards O<sub>2</sub><sup>•-</sup>, H<sub>2</sub>O<sub>2</sub>, and HOCl (51,52). Met<sup>329</sup> was the primary site of Met oxidation in albumin from human hepatocytes treated with AαC. The oxidation of Met residues, particularly Met<sup>329</sup>, has been observed in albumin of hemodialysis patients (52).

The major adducts of AαC formed with albumin were determined in human hepatocytes, by employing data-dependent scanning and bottom-up proteomics approaches, and the adduction products were the same as those adducts formed in vitro with commercial albumin reacted with N-oxidized AαC intermediates. The dose of AαC (50 μM) employed in human hepatocytes is greater than daily human exposure to AαC, but comparable to the doses employed in studies investigating the genotoxicity of AαC (18,19). The amount of AαC arising in mainstream smoke is 60 - 250 ng/cigarette (7,8). Thus, the intracellular or plasma levels of AαC found in humans exposed to this tobacco carcinogen are considerably lower than the amount of AαC

employed in our hepatocyte study. However, dG-C8-AαC formation occurs in a concentration-dependent manner in human hepatocytes treated with AαC over a 10,000-fold concentration range (1 nM – 10 μM), signifying that the reactive N-oxidation metabolites of AαC are formed at physiological exposure levels (20). More sensitive mass spectrometric-based methods are required for measuring AαC-albumin adducts and albumin oxidation products in hepatocytes at these lower exposure conditions to AαC.

The Cys<sup>34</sup> of albumin accounts for 80% of total free thiol content in plasma and considered a major antioxidant and scavenger of electrophiles in plasma (34). A number of genotoxicants and toxic electrophiles form adducts with the Cys<sup>34</sup> of rodent or human albumin (23). Many of these adducts have been characterized primarily in vitro and several adducts have been detected in humans. Albumin adducts have been identified with acrylamide (70), nitrogen mustard (71), α,β-unsaturated aldehydes (26), the neurotoxin brevetoxin B (72), acetaminophen (41), benzene (23), and several N-oxidized HAAs of diverse structures (32,35,56,73). In addition, aldehydes produced in tobacco smoke are scavenged by Cys<sup>34</sup> of albumin in vitro (74). Immunochemical techniques have shown carbonyl residues are formed with albumin exposed to cigarette smoke extract, and the carbonylation of albumin, by tobacco smoke, has been detected in lung tissue biopsy samples of smokers (75). Spectrophotometric assays have shown a decrease in the free Cys<sup>34</sup> content of albumin following exposure to cigarette smoke extracts in vitro (74,76). The diminution of free Cys<sup>34</sup> content may be attributed to adducts formed with aldehydes or by oxidation with ROS (26,74,77); however, a correlation between the level of adduct formation at Cys<sup>34</sup> of albumin and cigarette smoking constituents remains to be established in vivo. Recently, elevated levels of Cys<sup>34</sup>-SO<sub>2</sub>H of albumin were detected in plasma of smokers in a small pilot study (78). AαC, other HAAs, and structurally related aromatic amines present in tobacco smoke represent a class of chemicals in tobacco smoke that may contribute to the chemical modification or oxidation of Cys<sup>34</sup>, and the oxidation of Met residues of albumin.

In summary, AαC, a rodent liver carcinogen (12), undergoes bioactivation and forms adducts

with DNA and albumin, and induces oxidative stress in human hepatocytes. Albumin is a potent scavenger of ROS species generated by AαC metabolites. AαC, other HAAs, and many aromatic amines that arise in mainstream tobacco smoke (5,65,66) undergo N-oxidation in humans (54). Some of these metabolites form adducts with DNA and protein, and also induce oxidative stress, which may be contributing factors to liver damage and cancer risk in smokers. The Cys<sup>34</sup> adducts of N-oxidized HAAs and arylamines, or their hydrolysis products, and elevated levels of Cys<sup>34</sup>-SO<sub>2</sub>H and Cys<sup>34</sup>-SO<sub>3</sub>H of albumin may be potential biomarkers to assess exposure to these hazardous chemicals in tobacco smokers.

## REFERENCES

1. IARC. (1986) *IARC Monographs on the Evaluation of Carcinogenic Risks to Humans. Tobacco Smoking*, International Agency for Research on Cancer, Lyon, France
2. Luchtenborg, M., White, K. K., Wilkens, L., Kolonel, L. N., and Le Marchand, L. (2007) Smoking and colorectal cancer: different effects by type of cigarettes? *Cancer Epidemiol. Biomarkers Prev.* **16**, 1341-1347
3. Giovannucci, E. (2001) An updated review of the epidemiological evidence that cigarette smoking increases risk of colorectal cancer. *Cancer Epidemiol. Biomarkers Prev.* **10**, 725-731
4. Vineis, P., Alavanja, M., Buffler, P., Fontham, E., Franceschi, S., Gao, Y. T., Gupta, P. C., Hackshaw, A., Matos, E., Samet, J., Sitas, F., Smith, J., Stayner, L., Straif, K., Thun, M. J., Wichmann, H. E., Wu, A. H., Zaridze, D., Peto, R., and Doll, R. (2004) Tobacco and cancer: recent epidemiological evidence. *J. Natl. Cancer Inst.* **96**, 99-106
5. Hoffmann, D., Hoffmann, I., and El-Bayoumy, K. (2001) The less harmful cigarette: a controversial issue. a tribute to Ernst L. Wynder. *Chem. Res. Toxicol.* **14**, 767-790
6. Yoshida, D., Matsumoto, T., Yoshimura, R., and Matsuzaki, T. (1978) Mutagenicity of amino-alpha-carbolines in pyrolysis products of soybean globulin. *Biochem. Biophys. Res. Commun.* **83**, 915-920
7. Yoshida, D., and Matsumoto, T. (1980) Amino-alpha-carbolines as mutagenic agents in cigarette smoke condensate. *Cancer Lett.* **10**, 141-149
8. Zhang, L., Ashley, D. L., and Watson, C. H. (2011) Quantitative analysis of six heterocyclic aromatic amines in mainstream cigarette smoke condensate using isotope dilution liquid chromatography-electrospray ionization tandem mass spectrometry. *Nicotine.Tob.Res.* **13**, 120-126
9. IARC. (2002) *IARC Monographs on the Evaluation of Carcinogenic Risks to Humans. Tobacco smoke and involuntary smoking*, International Agency for Research on Cancer, Lyon, France
10. Kriek, E. (1992) Fifty years of research on N-acetyl-2-aminofluorene, one of the most versatile compounds in experimental cancer research. *J.Cancer Res.Clin.Oncol.* **118**, 481-489
11. Turesky, R. J., Yuan, J. M., Wang, R., Peterson, S., and Yu, M. C. (2007) Tobacco smoking and urinary levels of 2-amino-9H-pyrido[2,3-b]indole in men of Shanghai, China. *Cancer Epidemiol. Biomarkers Prev.* **16**, 1554-1560
12. Sugimura, T., Wakabayashi, K., Nakagama, H., and Nagao, M. (2004) Heterocyclic amines: Mutagens/carcinogens produced during cooking of meat and fish. *Cancer Sci.* **95**, 290-299
13. Okonogi, H., Ushijima, T., Shimizu, H., Sugimura, T., and Nagao, M. (1997) Induction of aberrant crypt foci in C57BL/6N mice by 2-amino-9H-pyrido[2,3-b]indole (A $\alpha$ C) and 2-amino-3,8-dimethylimidazo[4,5-f]quinoxaline (MeIQx). *Cancer Lett.* **111**, 105-109
14. Zhang, X. B., Felton, J. S., Tucker, J., Urlando, C., and Heddle, J. A. (1996) Intestinal mutagenicity of two carcinogenic food mutagens in transgenic mice: 2-amino-1-methyl-6-phenylimidazo [4,5-b] pyridine and amino( $\alpha$ )carboline. *Carcinogenesis* **17**, 2259-2265
15. Niwa, T., Yamazoe, Y., and Kato, R. (1982) Metabolic activation of 2-amino-9H-pyrido[2,3-b]indole by rat-liver microsomes. *Mutat. Res.* **95**, 159-170
16. Raza, H., King, R. S., Squires, R. B., Guengerich, F. P., Miller, D. W., Freeman, J. P., Lang, N. P., and Kadlubar, F. F. (1996) Metabolism of 2-amino-alpha-carboline. A food-borne heterocyclic amine mutagen and carcinogen by human and rodent liver microsomes and by human cytochrome P4501A2. *Drug Metab.Dispos.* **24**, 395-400
17. King, R. S., Teitel, C. H., and Kadlubar, F. F. (2000) In vitro bioactivation of N-hydroxy-2-amino-alpha-carboline. *Carcinogenesis* **21**, 1347-1354

18. Turesky, R. J., Bendaly, J., Yasa, I., Doll, M. A., and Hein, D. W. (2009) The impact of NAT2 acetylator genotype on mutagenesis and DNA adducts from 2-amino-9H-pyrido[2,3-*b*]indole. *Chem. Res. Toxicol.* **22**, 726-733
19. Majer, B. J., Kassie, F., Sasaki, Y., Pfau, W., Glatt, H., Meinl, W., Darroudi, F., and Knasmüller, S. (2004) Investigation of the genotoxic effects of 2-amino-9H-pyrido[2,3-*b*]indole in different organs of rodents and in human derived cells. *J. Chromatogr. B Analyt. Technol. Biomed. Life Sci.* **802**, 167-173
20. Nauwelaers, G., Bellamri, M., Fessard, V., Turesky, R. J., and Langouët, S. (2013) DNA adducts of the tobacco carcinogens 2-amino-9H-pyrido[2,3-*b*]indole and 4-aminobiphenyl are formed at environmental exposure levels and persist in human hepatocytes. *Chem. Res. Toxicol.* **26**, 1367-1377
21. Miller, J. A. (1970) Carcinogenesis by chemicals: an overview--G. H. A. Clowes memorial lecture. *Cancer Res.* **30**, 559-576
22. Tornqvist, M., Fred, C., Haglund, J., Helleberg, H., Paulsson, B., and Rydberg, P. (2002) Protein adducts: quantitative and qualitative aspects of their formation, analysis and applications. *J. Chromatogr. B Analyt. Technol. Biomed. Life Sci.* **778**, 279-308
23. Rappaport, S. M., Li, H., Grigoryan, H., Funk, W. E., and Williams, E. R. (2012) Adductomics: Characterizing exposures to reactive electrophiles. *Toxicol. Lett.* **213**, 83-90
24. Liebler, D. C. (2002) Proteomic approaches to characterize protein modifications: new tools to study the effects of environmental exposures. *Environ. Health Perspect.* **110 Suppl 1**, 3-9
25. Rubino, F. M., Pitton, M., Di, F. D., and Colombi, A. (2009) Toward an "omic" physiopathology of reactive chemicals: thirty years of mass spectrometric study of the protein adducts with endogenous and xenobiotic compounds. *Mass Spectrom. Rev.* **28**, 725-784
26. Aldini, G., Regazzoni, L., Orioli, M., Rimoldi, I., Facino, R. M., and Carini, M. (2008) A tandem MS precursor-ion scan approach to identify variable covalent modification of albumin Cys34: a new tool for studying vascular carbonylation. *J. Mass Spectrom.* **43**, 1470-1481
27. Skipper, P. L., and Tannenbaum, S. R. (1990) Protein adducts in the molecular dosimetry of chemical carcinogens. *Carcinogenesis* **11**, 507-518
28. Yu, M. C., Skipper, P. L., Tannenbaum, S. R., Chan, K. K., and Ross, R. K. (2002) Arylamine exposures and bladder cancer risk. *Mutat. Res.* **506-507**, 21-28
29. Peng, L., and Turesky, R. J. (2014) Optimizing proteolytic digestion conditions for the analysis of serum albumin adducts of 2-amino-1-methyl-6-phenylimidazo[4,5-*b*]pyridine, a potential human carcinogen formed in cooked meat. *J. Proteomics* **103**, 267-278
30. Peng, L., and Turesky, R. J. (2013) Capturing labile sulfenamide and sulfinamide serum albumin adducts of carcinogenic arylamines by chemical oxidation. *Anal. Chem.* **85**, 1065-1072
31. Westra, J. G. (1981) A rapid and simple synthesis of reactive metabolites of carcinogenic aromatic amines in high yield. *Carcinogenesis* **2**, 355-357
32. Peng, L., and Turesky, R. J. (2011) Mass spectrometric characterization of 2-amino-1-methyl-6-phenylimidazo[4,5-*b*]pyridine N-oxidized metabolites bound at Cys<sup>34</sup> of human serum albumin. *Chem. Res. Toxicol.* **24**, 2004-2017
33. Nauwelaers, G., Bessette, E. E., Gu, D., Tang, Y., Rageul, J., Fessard, V., Yuan, J. M., Yu, M. C., Langouët, S., and Turesky, R. J. (2011) DNA adduct formation of 4-aminobiphenyl and heterocyclic aromatic amines in human hepatocytes. *Chem. Res. Toxicol.* **24**, 913-925
34. Carballal, S., Radi, R., Kirk, M. C., Barnes, S., Freeman, B. A., and Alvarez, B. (2003) Sulfenic acid formation in human serum albumin by hydrogen peroxide and peroxyntirite. *Biochemistry* **42**, 9906-9914
35. Turesky, R. J., Skipper, P. L., and Tannenbaum, S. R. (1987) Binding of 2-amino-3-methylimidazo[4,5-*f*]quinoline to hemoglobin and albumin in vivo in the rat. Identification of an adduct suitable for dosimetry. *Carcinogenesis* **8**, 1537-1542

36. Turesky, R. J., and Markovic, J. (1994) DNA adduct formation of the food carcinogen 2-amino-3-methylimidazo[4,5-f]quinoline at the C-8 and N2 atoms of guanine. *Chem. Res. Toxicol.* **7**, 752-761
37. Langouët, S., Coles, B., Morel, F., Becquemont, L., Beaune, P., Guengerich, F. P., Ketterer, B., and Guillouzo, A. (1995) Inhibition of CYP1A2 and CYP3A4 by oltipraz results in reduction of aflatoxin B1 metabolism in human hepatocytes in primary culture. *Cancer Res.* **55**, 5574-5579
38. Tabb, D. L., Fernando, C. G., and Chambers, M. C. (2007) MyriMatch: highly accurate tandem mass spectral peptide identification by multivariate hypergeometric analysis. *J. Proteome. Res.* **6**, 654-661
39. Goodenough, A. K., Schut, H. A., and Turesky, R. J. (2007) Novel LC-ESI/MS/MS method for the characterization and quantification of 2'-deoxyguanosine adducts of the dietary carcinogen 2-amino-1-methyl-6-phenylimidazo[4,5-b]pyridine by 2-D linear quadrupole ion trap mass spectrometry. *Chem. Res. Toxicol.* **20**, 263-276
40. Tang, Y., Kassie, F., Qian, X., Ansha, B., and Turesky, R. J. (2013) DNA adduct formation of 2-amino-9H-pyrido[2,3-b]indole and 2-amino-3,4-dimethylimidazo[4,5-f]quinoline in mouse liver and extrahepatic tissues during a subchronic feeding study. *Toxicol. Sci.* **133**, 248-258
41. Damsten, M. C., Commandeur, J. N., Fidder, A., Hulst, A. G., Touw, D., Noort, D., and Vermeulen, N. P. (2007) Liquid chromatography/tandem mass spectrometry detection of covalent binding of acetaminophen to human serum albumin. *Drug Metab. Dispos.* **35**, 1408-1417
42. Kang, P., Dalvie, D., Smith, E., Zhou, S., and Deese, A. (2007) Identification of a novel glutathione conjugate of flutamide in incubations with human liver microsomes. *Drug Metab. Dispos.* **35**, 1081-1088
43. Saito, K., and Kato, R. (1984) Glutathione conjugation of aryl nitroso compound: detection and monitoring labile intermediates in situ inside a fast atom bombardment mass spectrometer. *Biochem. Biophys. Res. Commun.* **124**, 1-5
44. Eyer, P. G., P. (1996) Reaction of nitrosoarenes with SH groups. in *The chemistry of amine, nitroso, nitro and related groups. Part 1* (Patai, S. ed.), John Wiley & Sons, Chichester. pp 999-1040
45. Lemke, T. L. (2012) Review of Organic Functional Groups in *Introduction to Medicinal Organic Chemistry* Fifth Ed., Lippincott Williams & Wilkins, Baltimore, MD. pp 85-87
46. Novak, M., and Kazerani, S. (2000) Characterization of the 2-(α-carbolinyl)nitrenium ion and its conjugate base produced during the decomposition of the model carcinogen 2-N-(pivaloyloxy)-2-amino-α-carboline in aqueous solution. *J. Am. Chem. Soc.* **122**, 3606-3616
47. Steen, H., and Mann, M. (2001) Similarity between condensed phase and gas phase chemistry: fragmentation of peptides containing oxidized cysteine residues and its implications for proteomics. *J. Am. Soc. Mass Spectrom.* **12**, 228-232
48. Novak, M., and Nguyen, T. M. (2003) Unusual reactions of the model carcinogen N-acetoxy-N-acetyl-2-amino-α-carboline. *J. Org. Chem.* **68**, 9875-9881
49. Murata, M., and Kawanishi, S. (2011) Mechanisms of oxidative DNA damage induced by carcinogenic arylamines. *Front Biosci (Landmark Ed)* **16**, 1132-1143
50. Colombo, G., Clerici, M., Giustarini, D., Rossi, R., Milzani, A., and Dalle-Donne, I. (2012) Redox albuminomics: oxidized albumin in human diseases. *Antioxid. Redox Signal.* **17**, 1515-1527
51. Finch, J. W., Crouch, R. K., Knapp, D. R., and Schey, K. L. (1993) Mass spectrometric identification of modifications to human serum albumin treated with hydrogen peroxide. *Arch. Biochem. Biophys.* **305**, 595-599
52. Bruschi, M., Petretto, A., Candiano, G., Musante, L., Movilli, E., Santucci, L., Urbani, A., Gusmano, R., Verrina, E., Cancarini, G., Scolari, F., and Ghiggeri, G. M. (2008) Determination of the oxido-redox status of plasma albumin in hemodialysis patients. *J. Chromatogr. B Analyt. Technol. Biomed. Life Sci.* **864**, 29-37

53. Guillouzo, A. (1998) Liver cell models in in vitro toxicology. *Environ. Health Persp. (supplement)* **106**, 511-532
54. Turesky, R. J., and Le Marchand, L. (2011) Metabolism and biomarkers of heterocyclic aromatic amines in molecular epidemiology studies: lessons learned from aromatic amines. *Chem. Res. Toxicol.* **24**, 1169-1214
55. Felton, J. S., Jagerstad, M., Knize, M. G., Skog, K., and Wakabayashi, K. (2000) Contents in foods, beverages and tobacco. in *Food Borne Carcinogens Heterocyclic Amines* (Nagao, M., and Sugimura, T. eds.), John Wiley & Sons Ltd., Chichester, England. pp 31-71
56. Peng, L., Dasari, S., Tabb, D. L., and Turesky, R. J. (2012) Mapping serum albumin adducts of the food-borne carcinogen 2-amino-1-methyl-6-phenylimidazo[4,5-b]pyridine by data-dependent tandem mass spectrometry. *Chem. Res. Toxicol.* **25**, 2179-2193
57. John, H., Breyer, F., Thumfart, J. O., Hochstetter, H., and Thiermann, H. (2010) Matrix-assisted laser desorption/ionization time-of-flight mass spectrometry (MALDI-TOF MS) for detection and identification of albumin phosphorylation by organophosphorus pesticides and G- and V-type nerve agents. *Anal. Bioanal. Chem.* **398**, 2677-2691
58. Noort, D., Hulst, A. G., van, Z. A., van, R. E., and van der Schans, M. J. (2009) Covalent binding of organophosphorothioates to albumin: a new perspective for OP-pesticide biomonitoring? *Arch. Toxicol.* **83**, 1031-1036
59. Li, B., Schopfer, L. M., Hinrichs, S. H., Masson, P., and Lockridge, O. (2007) Matrix-assisted laser desorption/ionization time-of-flight mass spectrometry assay for organophosphorus toxicants bound to human albumin at Tyr411. *Anal. Biochem.* **361**, 263-272
60. Turesky, R. J., Rossi, S. C., Welti, D. H., Lay, J. J. O., and Kadlubar, F. F. (1992) Characterization of DNA adducts formed in vitro by reaction of N-hydroxy-2-amino-3-methylimidazo[4,5-f]quinoline and N-hydroxy-2-amino-3,8-dimethylimidazo[4,5-f]quinoxaline at the C-8 and N2 atoms of guanine. *Chem. Res. Toxicol.* **5**, 479-490
61. Snyderwine, E. G., Roller, P. P., Adamson, R. H., Sato, S., and Thorgeirsson, S. S. (1988) Reaction of the N-hydroxylamine and N-acetoxy derivatives of 2-amino-3-methylimidazo[4,5-f]quinoline with DNA. Synthesis and identification of N-(deoxyguanosin-8-yl)-IQ. *Carcinogenesis* **9**, 1061-1065
62. Frederiksen, H., Frandsen, H., and Pfau, W. (2004) Syntheses of DNA-adducts of two heterocyclic amines, 2-amino-3-methyl-9H-pyrido[2,3-b]indole (MeAaC) and 2-amino-9H-pyrido[2,3-b]indole (AaC) and identification of DNA-adducts in organs from rats dosed with MeAaC. *Carcinogenesis* **25**, 1525-1533
63. Bessette, E. E., Spivack, S. D., Goodenough, A. K., Wang, T., Pinto, S., Kadlubar, F. F., and Turesky, R. J. (2010) Identification of carcinogen DNA adducts in human saliva by linear quadrupole ion trap/multistage tandem mass spectrometry. *Chem. Res. Toxicol.* **23**, 1234-1244
64. Kim, D., Kadlubar, F. F., Teitel, C. H., and Guengerich, F. P. (2004) Formation and reduction of aryl and heterocyclic nitroso compounds and significance in the flux of hydroxylamines. *Chem. Res. Toxicol.* **17**, 529-536
65. IARC. (1986) *IARC Monographs on the Evaluation of Carcinogenic Risks to Humans: Tobacco smoking* International Agency for Research on Cancer, Lyon, France
66. Hecht, S. S. (2003) Tobacco carcinogens, their biomarkers and tobacco-induced cancer. *Nat. Rev. Cancer* **3**, 733-744
67. Siraki, A. G., Chan, T. S., Galati, G., Teng, S., and O'Brien, P. J. (2002) N-oxidation of aromatic amines by intracellular oxidases. *Drug Metab. Rev.* **34**, 549-564
68. Neumann, H. G. (2007) Aromatic amines in experimental cancer research: tissue-specific effects, an old problem and new solutions. *Crit. Rev. Toxicol.* **37**, 211-236
69. Tsuneoka, Y., Dalton, T. P., Miller, M. L., Clay, C. D., Shertzer, H. G., Talaska, G., Medvedovic, M., and Nebert, D. W. (2003) 4-aminobiphenyl-induced liver and urinary bladder DNA adduct formation in Cyp1a2(-/-) and Cyp1a2(+/-) mice. *J. Natl. Cancer Inst.* **95**, 1227-1237

70. Noort, D., Fidder, A., and Hulst, A. G. (2003) Modification of human serum albumin by acrylamide at cysteine-34: a basis for a rapid biomonitoring procedure. *Arch. Toxicol.* **77**, 543-545
71. Noort, D., Fidder, A., Hulst, A. G., Woolfitt, A. R., Ash, D., and Barr, J. R. (2004) Retrospective detection of exposure to sulfur mustard: improvements on an assay for liquid chromatography-tandem mass spectrometry analysis of albumin-sulfur mustard adducts. *J. Anal. Toxicol.* **28**, 333-338
72. Wang, Z., and Ramsdell, J. S. (2011) Analysis of interactions of brevetoxin-B and human serum albumin by liquid chromatography/mass spectrometry. *Chem. Res. Toxicol.* **24**, 54-64
73. Reistad, R., Frandsen, H., Grivas, S., and Alexander, J. (1994) In vitro formation and degradation of 2-amino-1-methyl-6-phenylimidazo[4,5-*b*]pyridine (PhIP) protein adducts. *Carcinogenesis* **15**, 2547-2552
74. Colombo, G., Aldini, G., Orioli, M., Giustarini, D., Gornati, R., Rossi, R., Colombo, R., Carini, M., Milzani, A., and Dalle-Donne, I. (2010) Water-Soluble alpha,beta-unsaturated aldehydes of cigarette smoke induce carbonylation of human serum albumin. *Antioxid.Redox.Signal.* **12**, 349-364
75. Hackett, T. L., Scarci, M., Zheng, L., Tan, W., Treasure, T., and Warner, J. A. (2010) Oxidative modification of albumin in the parenchymal lung tissue of current smokers with chronic obstructive pulmonary disease. *Respir. Res.* **11**, 180
76. Colombo, G., Rossi, R., Gagliano, N., Portinaro, N., Clerici, M., Annibal, A., Giustarini, D., Colombo, R., Milzani, A., and Dalle-Donne, I. (2012) Red blood cells protect albumin from cigarette smoke-induced oxidation. *PLoS One* **7**, e29930
77. Colzani, M., Aldini, G., and Carini, M. (2013) Mass spectrometric approaches for the identification and quantification of reactive carbonyl species protein adducts. *J. Proteomics* **92**, 28-50
78. Grigoryan, H., Li, H., Iavarone, A. T., Williams, E. R., and Rappaport, S. M. (2012) Cys<sup>34</sup> adducts of reactive oxygen species in human serum albumin. *Chem. Res. Toxicol.* **25**, 1633-1642

## FOOTNOTES

\*\*This work was supported by NIH grants RO1 CA134700 and R01CA134700-03S1 of the Family Smoking Prevention and Tobacco Control Act and the PNREST Anses, Cancer TMOI AVIESAN (2013/1/166).

<sup>1</sup>To whom correspondence should be addressed: Robert J. Turesky, Masonic Cancer Center and Department of Medicinal Chemistry, University of Minnesota, Minneapolis, MN 55455, USA, Tel.: (612) 626-0141; Fax: (612) 624-3869; E-mail: [rturesky@umn.edu](mailto:rturesky@umn.edu).

<sup>2</sup>The abbreviations used are: A $\alpha$ C, 2-Amino-9*H*-pyrido[2-3-*b*]indole; *N*-acetoxy-A $\alpha$ C, *N*-acetoxy-9*H*-pyrido[2-3-*b*]indole; HONH-A $\alpha$ C, 2-hydroxyamino-9*H*-pyrido[2-3-*b*]indole; NO-A $\alpha$ C, 2-nitroso-9*H*-pyrido[2-3-*b*]indole; NO<sub>2</sub>-A $\alpha$ C, 2-nitro-9*H*-pyrido[2-3-*b*]indole; P450, cytochrome P450; HAA, heterocyclic aromatic amines; Hb, hemoglobin; ; PhIP, 2-amino-1-methyl-6-phenylimidazo[4,5-*b*]pyridine;  $\beta$ ME  $\beta$ -mercaptoethanol; IAM, iodoacetamide; DMSO, dimethyl sulfoxide; SPE, solid phase extraction; THF, tetrahydrofuran; DDA, data dependent acquisition; MS/MS, tandem mass spectrometry; CID, collision induced dissociation; HCD, high-energy collision dissociation; UPLC, ultra performance liquid chromatography.





## FIGURE LEGENDS

**FIGURE 1.** Bioactivation of AαC, albumin adduct formation and induction of ROS in human hepatocytes. AαC undergoes bioactivation by P450 to form HONH-AαC. The HONH-AαC and its N-O esters react with albumin to form AαC-Cys<sup>34</sup> sulfenamide and sulfinamide adducts, and also react with DNA to form dG-C8-AαC. HONH-AαC can undergo further oxidation by P450, transition metals, or by oxygen to form NO-AαC and ROS. A redox cycling mechanism catalyzed by NADPH-P450 reductase can regenerate HONH-AαC (49,64). The superoxide anion or other ROS can oxidize S-N linked of Cys-AαC to form the sulfonamide linkage. The ROS generated by N-oxidized AαC also directly oxidize albumin to form the sulfinic and sulfonic acids of Cys<sup>34</sup> and Met residues of albumin.

**FIGURE 2.** Characterization of AαC and its N-oxidized metabolites. (A) UV spectra of AαC, NO-AαC and HONH-AαC were obtained in methanol. Product ion spectra of (B) AαC, (C) NO-AαC, and (D) HONH-AαC were acquired by ion trap mass spectrometry.

**FIGURE 3.** Mass tag data dependent MS<sup>2</sup> scanning of trypsin/chymotrypsin digest of albumin modified with 50 mol excess of an equimolar mixture of *N*-acetoxy-AαC and [<sup>13</sup>C<sub>6</sub>] *N*-acetoxy-AαC. Reconstructed ion chromatograms for AαC at *m/z* 183.1 and 184.1 from digests of albumin modified with *N*-acetoxy-AαC/ [<sup>13</sup>C<sub>6</sub>] *N*-acetoxy-AαC (upper panel), or digests of non-modified albumin (lower panel). The chromatograms were acquired on ions exhibiting mass difference of *m/z* 6 (for singly charged ions), *m/z* 3 (for doubly charged ions) and *m/z* 2 (for triply charged ions). The ion intensities were normalized to the same scale.

**FIGURE 4.** Product ion spectra of AαC adducts of (A) LQQC<sup>[SO<sub>2</sub>AαC]</sup>PFEDHVK (P2) [M+3H]<sup>3+</sup> at *m/z* 519.6, (B) LQQC<sup>[SOAαC]</sup>PFEDHVK (P3) [M+3H]<sup>3+</sup> at *m/z* 514.2, (C) Consecutive reaction monitoring at the MS<sup>3</sup> scan stage of LQQC<sup>[SOAαC]</sup>PFEDHVK (P3) targeting *m/z* 679.9 product ion from second generation product ion spectrum of *m/z* 514.2, (D) LQQC<sup>[SO<sub>2</sub>AαC]</sup>PF (P4) [M+2H]<sup>2+</sup> at *m/z* 474.7, (E) LQQC<sup>[SOAαC]</sup>PF (P7) [M+2H]<sup>2+</sup> at *m/z* 466.7, (F) third generation product ion spectrum of [M+2H]<sup>2+</sup> at *m/z* 466.7 > 750.4 > , and (G) LQQC<sup>[AαC]</sup>PF (P8) [M+2H]<sup>2+</sup> at *m/z* 658.7 of the trypsin/chymotrypsin digest of albumin modified with *N*-acetoxy-AαC and [<sup>13</sup>C<sub>6</sub>] *N*-acetoxy-AαC. \*denotes the fragment ions with AαC adduction.

**FIGURE 5.** AαC-Cys S-dioxide adducts of albumin obtained from pronase E/ prolidase/ leucine amino peptidase digest of albumin modified with HONH-AαC and [<sup>13</sup>C<sub>6</sub>] HONH-AαC or *N*-acetoxy-AαC and [<sup>13</sup>C<sub>6</sub>] *N*-acetoxy-AαC. Total ion chromatogram (TIC) at the MS<sup>2</sup> scan stage of [M+H]<sup>+</sup> at *m/z* 335.0806 obtained from albumin modified with (A) HONH-AαC and (B) *N*-acetoxy-AαC (lower panel). The product ion spectra of [M+H]<sup>+</sup> at *m/z* 335.0806 of C<sup>[SO<sub>2</sub>AαC]</sup> at (C) at 10.9 min and (D) at 11.5 min, and proposed structures of isomers are shown. (E) Proposed formation of Cysteine-S-yl-dioxide-AαC isomeric adducts by reaction of Cys with the nitrenium – carbenium ion resonance forms of HONH-AαC, and CID fragmentation mechanism of sulfonium ion at *m/z* 230.0385 in product ion spectra of isomers ([M+H]<sup>+</sup> at *m/z* 335.0806).

**FIGURE 6.** Product ion spectrum of AαC-Tyr peptide and mono amino acid adduct of albumin modified with *N*-acetoxy-AαC and [<sup>13</sup>C<sub>6</sub>] *N*-acetoxy-AαC. TIC, HCD and CID product ion spectra of (A)

LY<sup>[A $\alpha$ C]</sup>EIAR (P5) [M+2H]<sup>2+</sup> at  $m/z$  473.3,  $t_R$  14.1 min, (B) proposed CID fragmentation mechanism of LY<sup>[A $\alpha$ C]</sup>EIAR (P5) adduct [M+2H]<sup>2+</sup> at  $m/z$  473.3. (C) TIC and (D) product ion spectrum of [M+H]<sup>+</sup> at  $m/z$  363.1449 (A2) at  $t_R$  11.8 min, and (E) proposed CID fragmentation mechanism of A $\alpha$ C-Tyr adducts [M+H]<sup>+</sup> at  $m/z$  363.1452.

**FIGURE 7.** Characterization of isomeric FY<sup>[A $\alpha$ C]</sup>APELL peptides and an A $\alpha$ C-amine-linked Tyr amino acid adduct of albumin modified with *N*-acetoxy-A $\alpha$ C and [<sup>13</sup>C<sub>6</sub>] *N*-acetoxy-A $\alpha$ C. TIC, HCD and CID product ion spectra of (A) FY<sup>[A $\alpha$ C]</sup>APELL (P9) [M+2H]<sup>2+</sup> at  $m/z$  517.3,  $t_R$  14.5 min and 15.8 min (CID spectra for both peptides were identical, only the spectrum of peptide at  $t_R$  14.5 min is shown). (B) TIC and CID product ion spectra of A $\alpha$ C-amine-linked Tyr amino acid adduct [M+H]<sup>+</sup> at  $m/z$  361.1299 (A2) at  $t_R$  12.1 min. (C) Proposed CID fragmentation mechanism of A $\alpha$ C-Tyr adduct [M+H]<sup>+</sup> at  $m/z$  361.1299. \*Denotes the fragment ions with A $\alpha$ C adduction.

**FIGURE 8.** Ion counts of A $\alpha$ C-peptide adducts targeting at Cys<sup>34</sup> and Tyr<sup>140,150</sup> and free A $\alpha$ C recovered from trypsin/chymotrypsin digests of (A) albumin modified with 1/10<sup>-2</sup> molar equivalent of HONH-A $\alpha$ C or *N*-acetoxy-A $\alpha$ C, 0.3  $\mu$ g digest/injection (B) albumin modified with 1/10<sup>-4</sup> molar equivalent of HONH-A $\alpha$ C or *N*-acetoxy-A $\alpha$ C, 1.0  $\mu$ g digest/injection. Data are plotted as mean and standard deviation of ion counts (N = 3).

**FIGURE 9.** (A) Estimates of dG-C8-A $\alpha$ C adduct formation in hepatocytes of Donor A, B and C treated with 50  $\mu$ M of A $\alpha$ C. UPLC-ESI/MS<sup>3</sup> chromatograms of dG-C8-A $\alpha$ C from hepatocytes treated with 50  $\mu$ M A $\alpha$ C and with DMSO (control). For dG-C8-A $\alpha$ C, ions at  $m/z$  449.1 (MS) > 333.1 (MS<sup>2</sup>) > 209.2, 291.4, 316.4 (MS<sup>3</sup>) (upper level) and for the internal standard, [<sup>13</sup>C<sub>10</sub>]-dG-C8-A $\alpha$ C, ions at  $m/z$  459.1 (MS) > 338.1 (MS<sup>2</sup>) > 210.2, 295.4, 321.5 (MS<sup>3</sup>) (lower level) were monitored. (B) UPLC-ESI/MS<sup>2</sup> chromatograms of A $\alpha$ C-peptide adducts and Cys and Met oxidation products recovered from trypsin/chymotrypsin digests of albumin from hepatocytes of Donor A treated with A $\alpha$ C and [<sup>13</sup>C<sub>6</sub>] A $\alpha$ C (50  $\mu$ M) and Donor A treated with DMSO (Control). Ion counts of (C) A $\alpha$ C-peptide adducts and A $\alpha$ C, (D) Cys<sup>34</sup> sulfinic acid, Cys<sup>34</sup> sulfonic acid, Met<sup>329</sup> sulfoxide, and LQQC<sup>34</sup>PF alkylated with IAM obtained from trypsin/chymotrypsin digests of albumin of hepatocytes of Donor A, B and C treated with 50  $\mu$ M equimolar mixture of A $\alpha$ C and [<sup>13</sup>C<sub>6</sub>] A $\alpha$ C for 24 h or treated with DMSO (control). (Values are reported as the mean and standard deviation, N=3). \*P < 0.01 using one way ANOVA for Donors A, B and C treated with 50  $\mu$ M of A $\alpha$ C, \*\*P < 0.05 for comparison between Donor A to B and Donor B to C using Tukey's multiple comparison test for DNA adducts. \*P < 0.01 and \*\*P < 0.05 A $\alpha$ C treated versus control (DMSO treated) (2-tailed *t* test) for peptide adducts.

TABLE 1 AαC-peptide adducts identified using mass-tag data dependent acquisition

Peptide	Unlabeled ( <sup>13</sup> C <sub>6</sub> labeled) Observed precursor ions ( <i>m/z</i> )	Z	M.W	<i>t<sub>R</sub></i> (min)	AαC-peptide adduct	Site of modification	Enzyme
P1	481.9 (483.9)	3	1442.6	16.5	<sup>32</sup> QQ*C <sup>[AαC]</sup> PFEDHVK <sup>41</sup> sulfonamide <sup>a,b,c</sup>	Cys <sup>34</sup>	
P2	778.9 (781.9)	2	1555.7	17.7	<sup>31</sup> LQQ*C <sup>[AαC]</sup> PFEDHVK <sup>41</sup> sulfonamide <sup>a,b,c</sup>	Cys <sup>34</sup>	
	519.6 (521.6)	3					
P3	770.9 (773.9)	2	1539.7	17.8	<sup>31</sup> LQQ*C <sup>[AαC]</sup> PFEDHVK <sup>41</sup> sulfonamide <sup>a,b,c</sup>	Cys <sup>34</sup>	
	514.2 (516.3)	3					
P4	948.4 (954.4)	1	947.4	17.9	<sup>31</sup> LQQ*C <sup>[AαC]</sup> PF <sup>37</sup> sulfonamide <sup>a,b,c</sup>	Cys <sup>34</sup>	Trypsin- chymotrypsin
	474.4 (477.4)	2					
P5	473.3 (476.3)	2	944.5	19.0	<sup>139</sup> L*Y <sup>[AαC]</sup> EIAR <sup>144 a,b</sup>	Tyr <sup>140</sup>	
P6	616.8 (619.8)	2	1231.5	19.3	<sup>327</sup> LGM <sup>oxi</sup> FL*Y <sup>[AαC]</sup> EY <sup>334 a,b</sup>	Tyr <sup>332</sup>	
P7	932.4 (938.4)	1	931.4	20.4	<sup>31</sup> LQQ*C <sup>[AαC]</sup> PF <sup>37</sup> sulfonamide <sup>a,b,c</sup>	Cys <sup>34</sup>	
	466.7(469.7)	2					
P8	916.4 (922.4)	1	915.4	21.5	<sup>31</sup> LQQ*C <sup>[AαC]</sup> PF <sup>37</sup> sulfenamide <sup>a,b,c</sup>	Cys <sup>34</sup>	
	458.7 (461.7)	2					
P9(A,B)	517.3 (520.3)	2	1032.5	22.8	<sup>149</sup> F*Y <sup>[AαC]</sup> APELL <sup>155a,b,c</sup>	Tyr <sup>150</sup>	
Amino Acid	Unlabeled ( <sup>13</sup> C <sub>6</sub> labeled) Observed precursor ions ( <i>m/z</i> )	Z	M.W	<i>t<sub>R</sub></i> (min)	AαC-amino acid adduct	Site of modification	Enzyme
A1	335.0804 (341.0986)	1	335.1	10.9	*Cys <sup>[AαC]</sup> <sup>a,b</sup>	Cys	
A2	363.1449 (369.1631)	1	363.2	11.8	*Tyr <sup>[AαC]</sup> <sup>a,b</sup>	Tyr	3-Enzyme mixture
A3	361.1293 (367.1475)	1	361.1	12.1	*Tyr <sup>[AαC]</sup> <sup>a,b</sup>	Tyr	

Z – Charge state; *t<sub>R</sub>*- Retention time; M.W- Molecular weight; <sup>a</sup> HONH-AαC/ HONH-[<sup>13</sup>C<sub>6</sub>]AαC-albumin modified sample; <sup>b</sup> N-acetoxy-AαC/ N-acetoxy-[<sup>13</sup>C<sub>6</sub>]-AαC-albumin modified sample; <sup>c</sup> NO-AαC- modified sample; 3-Enzyme mixture: pronase E, leucine aminopeptidase, and prolidase.

**Table 2** Accurate mass measurements of AαC amino acid adducts formed with Tyr and Cys

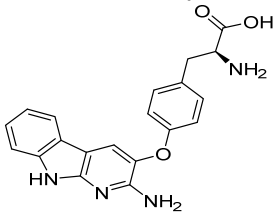
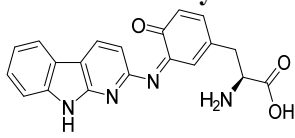
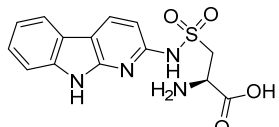
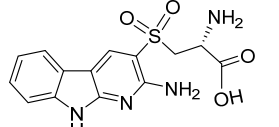
AαC-amino acid adduct	Precursor ion/product ion assignment	Observed <i>m/z</i>	Molecular Formula	Calculated <i>m/z</i>	Error ppm
<b>AαC-O-Tyr</b> 	[M+H] <sup>+</sup>	363.1449	C <sub>20</sub> H <sub>19</sub> N <sub>4</sub> O <sub>3</sub>	363.1451	0.5
	[M+H-H <sub>3</sub> N] <sup>+</sup>	346.1184	C <sub>20</sub> H <sub>16</sub> N <sub>3</sub> O <sub>3</sub>	346.1186	0.5
	[M+H-CH <sub>2</sub> O <sub>2</sub> ] <sup>+</sup>	317.1392	C <sub>19</sub> H <sub>17</sub> N <sub>4</sub> O	317.1396	1.0
	[M+H-CH <sub>3</sub> NO <sub>2</sub> ] <sup>+</sup>	302.1285	C <sub>19</sub> H <sub>16</sub> N <sub>3</sub> O	302.1287	0.7
	[M+H-C <sub>2</sub> H <sub>5</sub> NO <sub>2</sub> ] <sup>+</sup>	288.1129	C <sub>18</sub> H <sub>14</sub> N <sub>3</sub> O	288.1131	0.7
	[M+H-C <sub>9</sub> H <sub>11</sub> NO <sub>2</sub> ] <sup>+</sup>	198.0659	C <sub>11</sub> H <sub>8</sub> N <sub>3</sub> O	198.0662	1.0
	[M+H-C <sub>9</sub> H <sub>10</sub> NO <sub>3</sub> ] <sup>+</sup>	183.0789	C <sub>11</sub> H <sub>9</sub> N <sub>3</sub>	183.0791	1.1
<b>AαC-N=Tyr</b> 	[M+H] <sup>+</sup>	361.1293	C <sub>20</sub> H <sub>17</sub> N <sub>4</sub> O <sub>3</sub>	361.1295	0.6
	[M+H-H <sub>3</sub> N] <sup>+</sup>	344.1025	C <sub>20</sub> H <sub>14</sub> N <sub>3</sub> O <sub>3</sub>	344.1029	1.1
	[M+H-CH <sub>2</sub> O <sub>2</sub> ] <sup>+</sup>	315.1239	C <sub>19</sub> H <sub>15</sub> N <sub>4</sub> O	315.1240	0.7
	[M+H-CH <sub>3</sub> NO <sub>2</sub> ] <sup>+</sup>	300.1130	C <sub>19</sub> H <sub>14</sub> N <sub>3</sub> O	300.1131	0.7
	[M+H-C <sub>2</sub> H <sub>5</sub> NO <sub>2</sub> ] <sup>+</sup>	288.1129	C <sub>18</sub> H <sub>14</sub> N <sub>3</sub> O	288.1137	2.8
	[M+H-C <sub>9</sub> H <sub>7</sub> NO <sub>3</sub> ] <sup>+</sup>	183.0789	C <sub>11</sub> H <sub>9</sub> N <sub>3</sub>	183.0791	1.1
	[M+H-C <sub>9</sub> H <sub>7</sub> NO <sub>3</sub> ] <sup>+</sup>	184.0868	C <sub>11</sub> H <sub>10</sub> N <sub>3</sub>	184.0869	0.5
<b>AαC-HN-SO<sub>2</sub>-Cys</b> 	[M+H] <sup>+</sup>	335.0804	C <sub>14</sub> H <sub>15</sub> N <sub>4</sub> O <sub>4</sub> S	335.0808	1.2
	[M+H-H <sub>3</sub> N] <sup>+</sup>	318.0546	C <sub>14</sub> H <sub>12</sub> N <sub>3</sub> O <sub>4</sub> S	318.0548	1.2
	[M+H-O <sub>2</sub> S] <sup>+</sup>	271.1193	C <sub>14</sub> H <sub>15</sub> N <sub>4</sub> O <sub>2</sub>	271.1190	0.4
	[M+H-H <sub>3</sub> NO <sub>2</sub> S] <sup>+</sup>	254.0928	C <sub>14</sub> H <sub>12</sub> N <sub>3</sub> O <sub>2</sub>	254.0924	-1.5
<b>AαC-SO<sub>2</sub>-Cys</b> 	[M+H-C <sub>3</sub> H <sub>12</sub> NO <sub>3</sub> ] <sup>+</sup>	230.0385	C <sub>11</sub> H <sub>3</sub> N <sub>3</sub> OS	230.0384	0.3
	[M+H-C <sub>3</sub> H <sub>5</sub> O <sub>4</sub> NS] <sup>+</sup>	184.0867	C <sub>11</sub> H <sub>10</sub> N <sub>3</sub>	184.0869	1.0
	[M+H-C <sub>3</sub> H <sub>6</sub> O <sub>4</sub> NS] <sup>+</sup>	183.0790	C <sub>11</sub> H <sub>9</sub> N <sub>3</sub>	183.0791	0.5

Figure 1

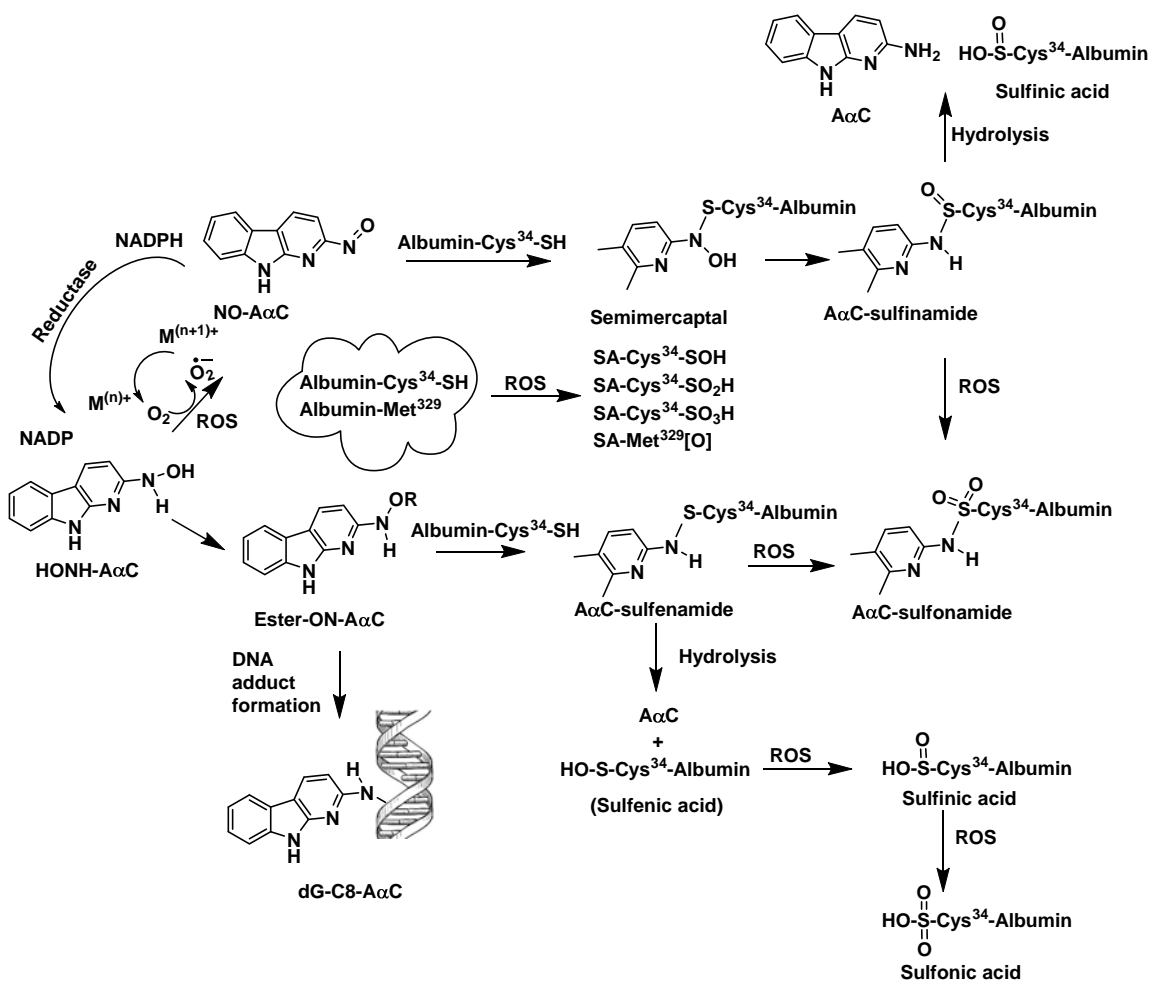


Figure 2

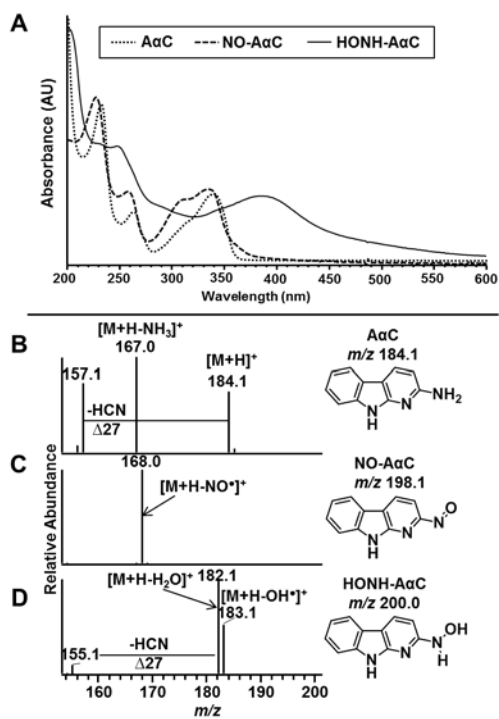


Figure 3

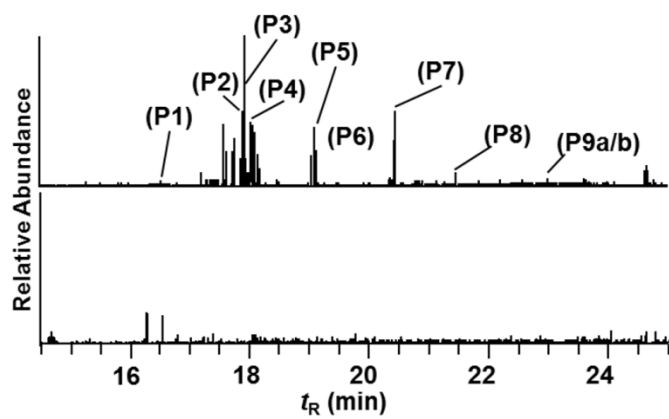




Figure 4

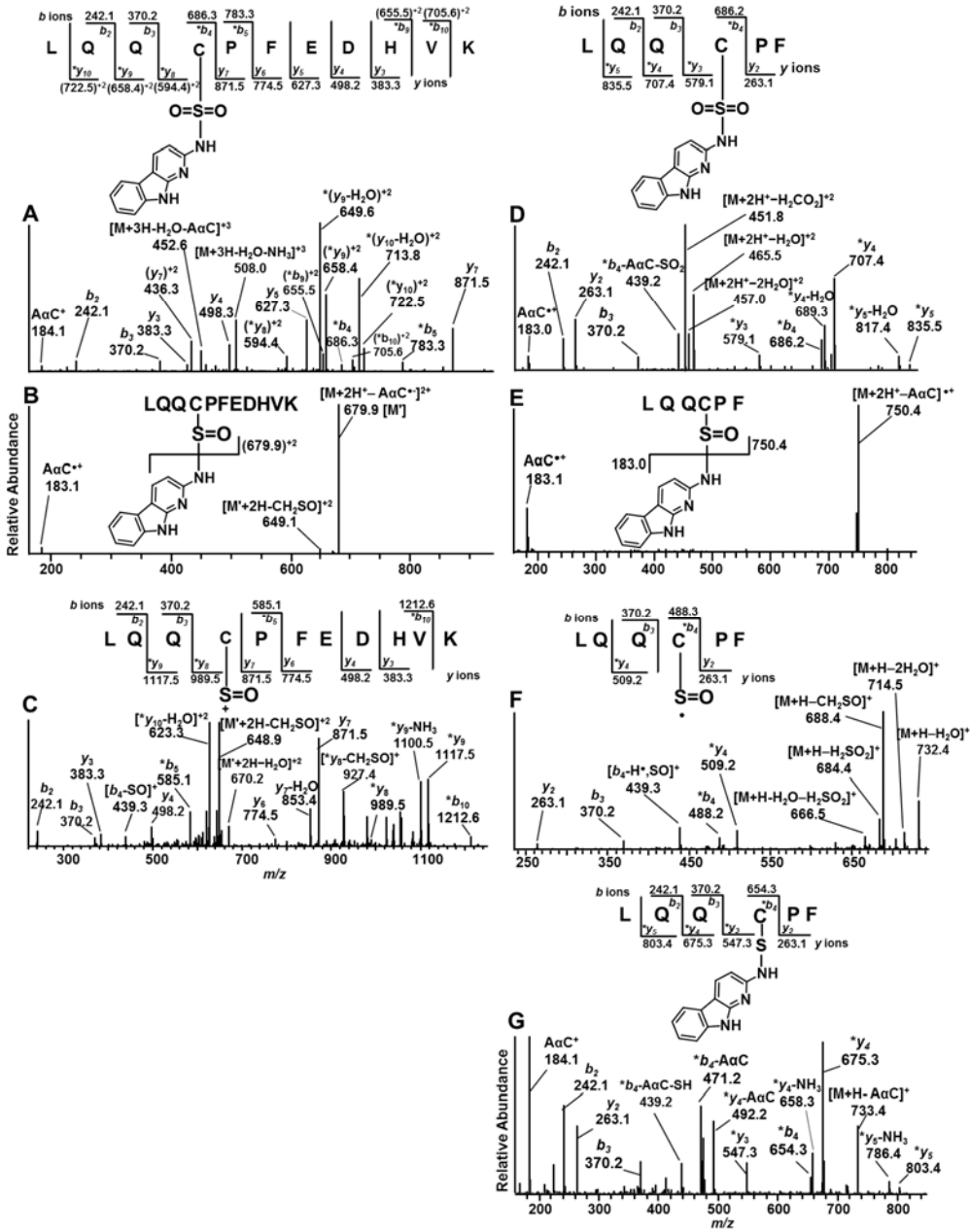


Figure 5

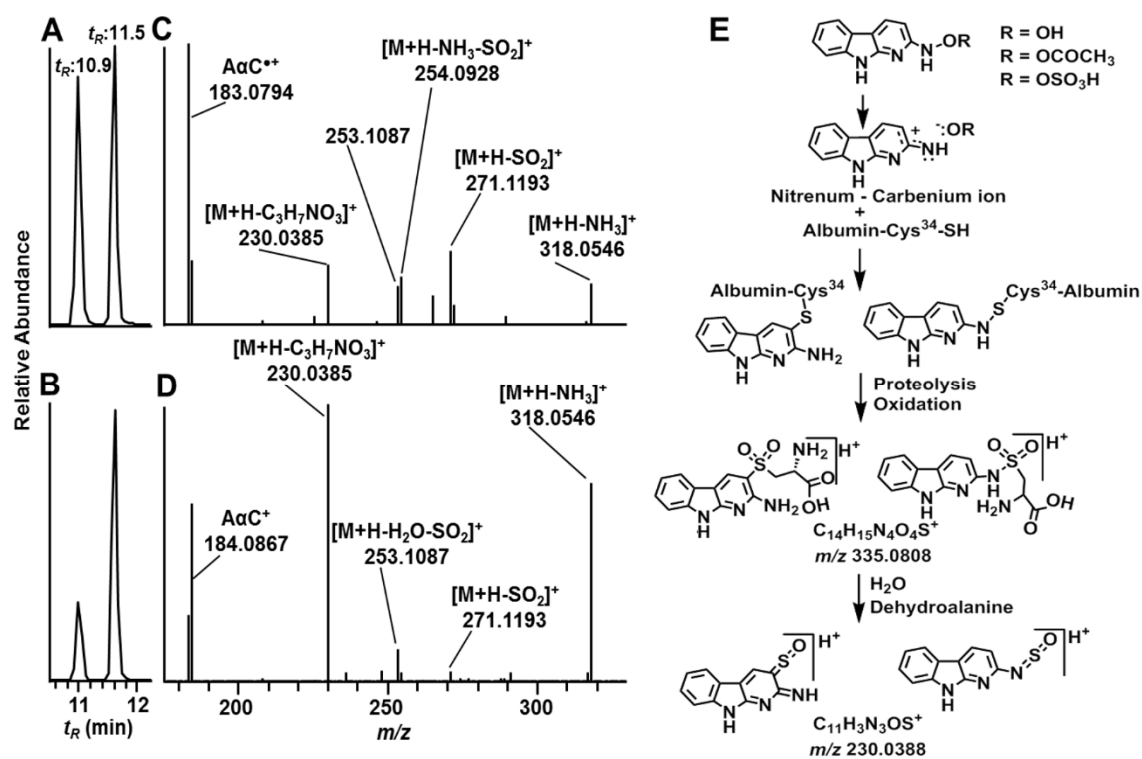


Figure 6

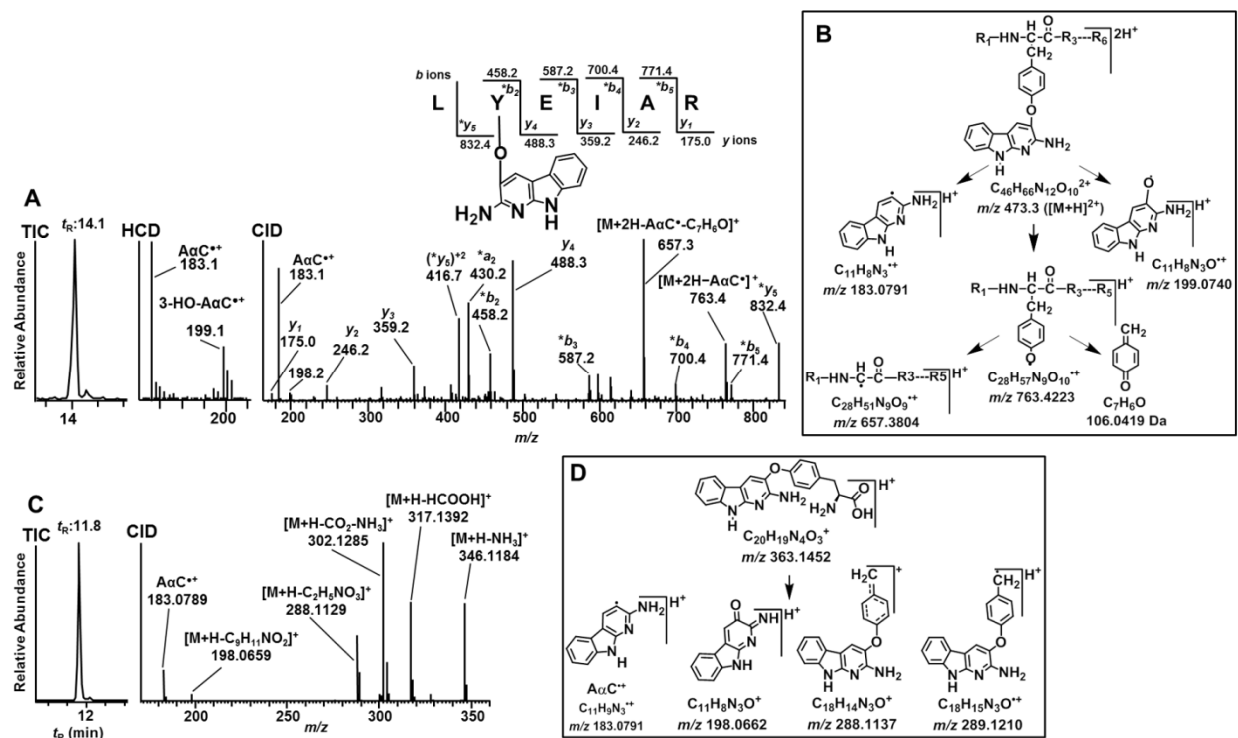


Figure 7

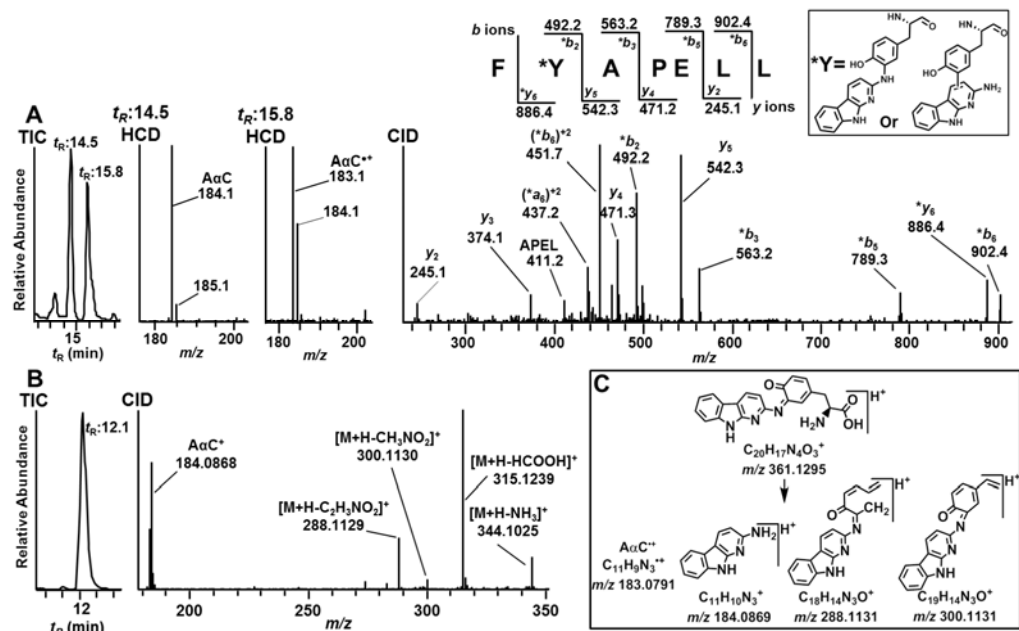


Figure 8

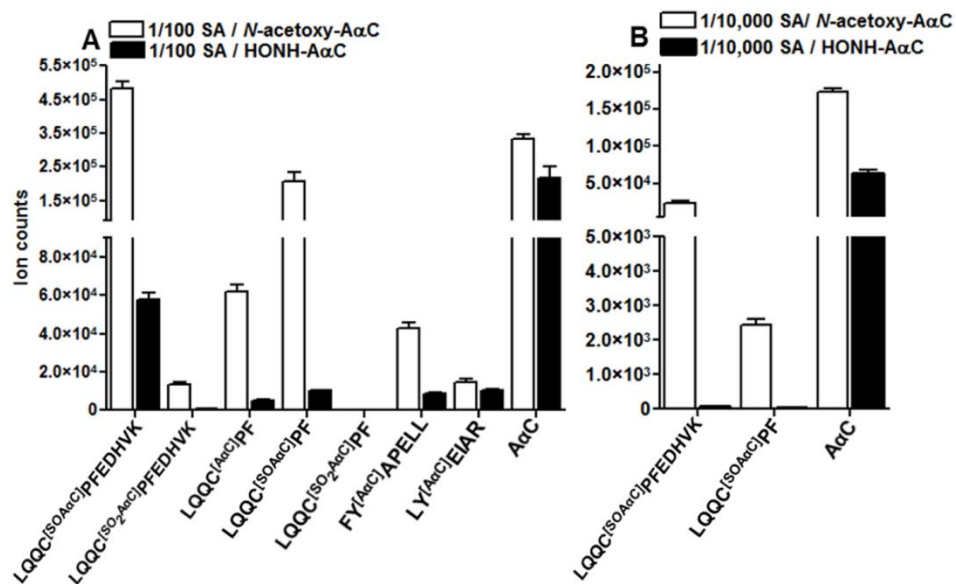


Figure 9

